UNIVERSITY OF TURKU

NOVEL ASPECTS OF INSULIN RESISTANCE: FOCUS ON THE BRAIN

Studies using positron emission tomography

Eleni Rebelos

TURUN YLIOPISTON JULKAISUJA – ANNALES UNIVERSITATIS TURKUENSIS
SARJA - SER. D OSA - TOM. 1498 | MEDICA - ODONTOLOGICA | TURKU 2020

UNIVERSITY OF TURKU

NOVEL ASPECTS OF INSULIN RESISTANCE: FOCUS ON THE BRAIN

Studies using positron emission tomography

Eleni Rebelos

TURUN YLIOPISTON JULKAISUJA – ANNALES UNIVERSITATIS TURKUENSIS
SARJA – SER. D OSA – TOM. 1498 | MEDICA – ODONTOLOGICA | TURKU 2020

University of Turku

Faculty of Medicine
Internal Medicine
Doctoral Program in Clinical Research
Turku PET Centre
Turku, Finland

Supervised by

Professor Pirjo Nuutila, MD, Ph.D
Turku PET Centre
University of Turku
Department of Endocrinology
Turku University Hospital
Turku, Finland

Docent Riikka Lautamäki, MD, Ph.D
Heart Centre
Turku University Hospital
Turku, Finland

Professor Ele Ferrannini, MD
Centro Nazionale di Ricerca (CNR)
Pisa, Italy

Reviewed by

Associate Professor
Vera Schrauwen-Hinderling, Ph.D
Department of Nutrition and Movement Sciences
Maastricht University
Maastricht, The Netherlands

Professor Riccardo Bonadonna, MD
Division of Endocrinology and Metabolic Diseases
University of Parma School of Medicine
Parma, Italy

Opponent

Professor Mikael Rydén, MD, Ph.D
Department of Medicine
Karolinska Institute
Karolinska, Sweden

The originality of this publication has been checked in accordance with the University of Turku quality assurance system using the Turnitin Origiality Check service.

ISBN 978-951-29-8150-2 (PRINT)
ISBN 978-951-29-8151-9 (PDF)
ISSN 0355-9483 (Print)
ISSN 2343-3213 (Online)
Painosalama Oy, Turku, Finland 2020

To my family

UNIVERSITY OF TURKU
Faculty of Medicine
Internal Medicine
ELENI REBELOS: Novel Aspects of Insulin Resistance: Focus on the Brain. Studies using positron emission tomography.
Academic dissertation, 125 pp.
Doctoral Program in Clinical Research
September 2020

ABSTRACT

We are currently facing a global epidemic of obesity, which poses a great challenge for the global health. Insulin resistance is the common soil that links obesity and type 2 diabetes. Whereas most lifestyle interventions fail, bariatric surgery has been a powerful weapon in the battle against obesity. Preclinical data have shown that the brain may directly control the determinants of glucose tolerance, namely insulin sensitivity and insulin secretion. We used positron emission tomography, to study whether brain metabolism assessed as brain glucose and/or brain fatty acid uptake is related to the endogenous glucose production (EGP), and ß-cell function. Moreover, we addressed whether there are differences in brain fatty acid uptake between morbidly obese and lean individuals as well as the effect of significant weight loss induced by bariatric surgery. Finally, we investigated whether brain substrate handling predicted any metabolic outcome at follow-up.

We found that in morbidly obese subjects brain glucose uptake (BGU) correlated positively with EGP, and that this association remained significant also six months after surgery. On the contrary, there was no such association in the lean subjects. In 52 non-diabetic subjects to whom ß-cell modeling was performed, insulin-stimulated BGU correlated also with the basal insulin secretion, total insulin output and potentiation of glucose-stimulated insulin secretion. Contrastingly, in 15 patients with type 2 diabetes BGU and insulin secretion did not correlate, but there was a significant inverse correlation between BGU and potentiation. Cross-sectionally in 34 studied women, brain fatty acid uptake (BFAU) also correlated negatively with potentiation, and similar trends were seen both in non-diabetics and diabetics.

Finally, we found that, unlike in lean individuals, BFAU is increased in morbidly obese subjects, and that six months after bariatric surgery, BFAU remained unchanged. Baseline BGU and baseline BFAU predicted worse glucose control at two-year follow-up after bariatric surgery.

In conclusion, this thesis work shows that brain substrate handling differs in obese and lean individuals and that brain metabolism may be a direct way of controlling whole-body homeostasis in humans. Moreover, in two different datasets, increased brain substrate uptake at baseline predicted worse metabolic outcome after bariatric surgery.

KEYWORDS: endogenous glucose production, β-cell function, brain glucose uptake, brain fatty acid uptake, bariatric surgery, positron emission tomography

TURUN YLIOPISTO
Lääketieteellinen tiedekunta
Sisätautioppi
ELENI REBELOS: Uusia löydöksia insuliiniresistenssiä koskien- tarkastelun kohteena aivot. Tutkimuksia positroniemissiotomografialla
Väiröskirja, 125 s.
Turun kliininen tohtoriohjelma
Syyskuu 2020

TIIVISTELMÄ

Tämänhetkinen lihavuusepidemia asettaa valtavan maailmanlaajuisen terveyshaasteen. Insuliiniresistenssi yhdistää lihavuuden tyypin 2 diabetekseen. Siinä missä elämäntapainterventiot useimmiten epäonnistuvat, lihavuusleikkaus on ollut tehokas ase lihavuuden vastaisessa taistelussa. Prekliinisten tutkimusten perusteella on osoitettu, että aivot voivat olla suoraan vastuussa insuliiniherkkyyden ja insuliinierityksen säätelystä ja siten glukoositasapainosta. Tutkimme positroniemissiotomografian avulla, onko aivojen glukoosin tai rasvahappojen otto yhteydessä kehon glukoosintuotantoon tai β-solujen toimintaan ihmisillä. Lisäksi selvitimme, ennustaako aivojen ravintoaineiden käsittely aineenvaihduntaan liittyviä muuttujia leikkauksen jälkeisen seurantajakson aikana.

Tutkimuksessa havaitsimme, että vaikeasti lihavilla tutkittavilla aivojen glukoosinotto korreloi positiivisesti kehon glukoosintuoton kanssa ja tämä yhteys säilyi myös 6 kk kuluttua leikkauksesta. Sitä vastoin normaalipainoisilla tutkittavilla tällaista yhteyttä ei havaittu. β-solujen toimintaa mallinnettiin 67:llä tutkittavalla. Analyysin perusteella aivojen glukoosinotolla oli positiivinen korrelaatio insuliinin perustilan tuotantoon, insuliinin kokonaistuotantoon sekä insuliinintuoton tehostamiseen. Sen sijaan aivojen rasvahappojen otto korreloi negatiivisesti insuliinintuoton tehostamiseen.

Tutkimuksessa havaittiin lisäksi, että aivojen rasvahappojenotto oli lisääntynyt vaikeasti lihavilla tutkittavilla normaalipainoisiin verrattuna ja tämä ero säilyi myös 6 kk leikkauksen jälkeen. Korkeampi aivojen glukoosin ja rasvahappojen otto ennen leikkausta ennusti huonompaa glukoositasapainoa 2 vuoden kuluttua leikkauksesta.

Tässä väitöstyössä osoitettiin, että aivojen aineenvaihdunta voi suoraan säädellä koko kehon aineenvaihduntaa. Lisäksi osoitettiin kahdessa erillisessä aineistossa suuremman aivojen ravintoaineiden oton ennustavan huonompaa aineenvaihdunnan terveyttä lihavuusleikkauksen jälkeen.

AVAINSANAT: endogeeninen glukoosin tuotanto, β-solujen toiminta, aivojen glukoosinotto, aivojen rasvahappojenotto, lihavuus, lihavuusleikkaus, positroniemissiotomografia

Table of Contents

Abbreviations

[^{18}F]FDG	[^{18}F]2-fluoro-2-deoxy-D-glucose
[^{18}F]FTHA	14(R,S)-[^{18}F]fluoro-6-thia-heptadecanoic acid
Aβ	amyloid beta
AD	Alzheimer disease
AUC	area under the curve
BBB	blood-brain barrier
BGU	brain glucose uptake
BFAU	brain fatty acid uptake
BMI	body mass index
BS	bariatric surgery
CBF	cerebral blood flow
$CMRO_2$	cerebral metabolic rate for oxygen
CNS	central nervous system
Cp	plasma concentration
DIO	diet-induced obesity
EGP	endogenous glucose production
FDR	false discovery rate
FA	fatty acids
FATP	fatty-acid transporter
FFA	free fatty acids
FLAIR	fluid-attenuated inversion recovery
FUR	fractional uptake rate
GFAP	glial fibrillary acidic protein
GIP	glucose dependent insulinotropic polypeptide
GIR	glucose infusion rate
GLP-1	glucagon-like peptide 1
HFD	high fat diet
HGP	hepatic glucose production
ICC	intraclass correlation coefficient
ICV	into the third-cerebral-ventricle
IFG	impaired fasting glucose

IGF-1	insulin-like growth factor 1
IGF-1R	insulin-like growth factor 1 receptor
IGT	impaired glucose tolerance
IQR	interquartile range
IR	insulin receptor
ISR	insulin secretion rate
IRS1	insulin receptor substrate 1
Ki	influx constant rate
LSG	laparoscopic Sleeve gastrectomy
MAP	mitogen-activated protein
MBH	mediobasal hypothalamus
MCT	monocarboxylate transporters
MNI	Montreal Neurological Institute
MRI	magnetic resonance imaging
MRS	magnetic resonance spectroscopy
NGT	normal glucose tolerance
NMR	nuclear magnetic resonance
NIRKO	neuron-specific IR knockout
non-T2D	subjects not affected by T2D
OGTT	oral glucose tolerance test
PET	positron emission tomography
PI3K	phosphatidylinositol-3-kinase
R_d	rate of disappearance
ROI	region of interest
RYGB	Roux-y gastric bypass
SUV	standardized uptake value
SPM	statistical parametric mapping
T2D	type 2 diabetes
WHP	waist-to-hip ratio

List of Original Publications

This dissertation is based on the following original publications, which are referred to in the text by their Roman numerals:

I Rebelos E, Immonen H, Bucci M, Hannukainen JC, Nummenmaa L, Honka MJ, Soinio M, Salminen P, Ferrannini E, Iozzo P, Nuutila P. 2019 Brain glucose uptake is associated with endogenous glucose production in obese patients before and after bariatric surgery and predicts metabolic outcome at follow-up. *Diabetes Obes Metab* 2019;21:218–226.

II Rebelos E, Mari A, Bucci M, Honka MJ, Hannukainen JC, Virtanen KA, Hirvonen J, Nummenmaa L, Heni M, Iozzo P, Ferrannini E, Nuutila P. Brain substrate metabolism and ß-cell function in humans: a positron emission tomography study. *Endocrinol Diabetes Metab* 2020;3:e00136.

III Rebelos E, Hirvonen J, Bucci M, Pekkarinen L, Nyman M, Hannukainen JC, Iozzo P, Salminen P, Nummenmaa L, Ferrannini E, Nuutila P. Brain FFA uptake is higher in morbidly obese as compared to lean subjects, and is attenuated after bariatric surgery: a positron emission tomography study. *Diabetes Obes Metab* 2020;22:1074-1082.

1 Introduction

Obesity is a rapidly increasing public health problem. We are currently facing a global obesity epidemic and the number of overweight and obese adults is projected to be 1.35 billion and 573 million, respectively, by 2030 (Kelly et al., 2008). Obesity is a major public health burden since it associates with an enhanced risk of cardiovascular disease, type 2 diabetes (T2D), stroke, neurodegenerative diseases, and many types of cancer (Pugazhenthi et al., 2017; World Health 2018). Obesity is strongly related to insulin resistance and T2D (Vazquez et al., 2007). The term "*diabesity*" was coined to underline the close pathophysiological connection between the two conditions.

Diet modification, and lifestyle intervention have proved to be only a weak arm in the fight against obesity, a condition of which the pathophysiology is much more complex than just overeating. Bariatric surgery, on the other hand, is the most powerful weapon in the battle against morbid obesity. As such, it is often used in a research setting in order to achieve rapid weight loss and marked improvement in insulin sensitivity.

Positron emission tomography (PET) is considered, nowadays, the gold standard for measuring regional substrate utilization in humans. With the application of PET, measuring metabolism at the tissue level is possible.

Previous studies from our centre using PET have shown that during euglycemic hyperinsulinemia obese subjects, and subjects with impaired glucose tolerance (IGT) have increased brain glucose uptake (BGU) compared to lean and normal glucose tolerant (NGT) individuals (Hirvonen et al., 2011; Tuulari et al., 2013). Even though this finding has been consolidated also from later studies from us and other groups in both animals and humans (Bahri et al., 2018; Latva-Rasku et al., 2017), its molecular mechanism remains unknown. A previous study from our centre also showed that brain fatty acid uptake is higher in subjects with metabolic syndrome (Karmi et al., 2010) than healthy, lean individuals.

In the present thesis, we sought to determine whether brain substrate uptake in obese, insulin resistant subjects relates also to other parameters of whole-body homeostasis (insulin sensitivity, endogenous glucose production, insulin secretion and other parameters of ß-cell function), and whether this increased brain substrate

uptake in insulin resistance can predict any metabolic outcome during follow-up. It is also worth mentioning that during the work performed for this PhD thesis, a novel idea has been conceived on the mechanism behind the increased BGU in obese/insulin resistant subjects. Even though such studies (on the mechanism) are not part of this PhD thesis, the study hypothesis is briefly described in this book.

2 Review of the Literature

2.1 Obesity and Insulin Resistance

Obesity is globally on the rise, more than 1.3 billion adults being overweight, and over 500 million being obese (Nguyen and El-Serag 2010). Obesity results in an increased risk for premature death and is the leading cause of a multitude of diseases: T2D, hypertension, dyslipidemia, asthma, arthritis and musculoskeletal disorders as well as many types of cancer (Mokdad et al., 2003). Obesity is also linked to an increased vulnerability to infectious diseases, such as the SARS-COV2, which caused the recent pandemic (Moriconi et al., 2020; Rebelos et al., 2020b).

In 2011 there were approximately 366 million people with T2D, and this number is expected to rise to 552 million by 2030 (Whiting et al., 2011).

The common link between obesity and T2D is insulin resistance. Initially, the ß-cells are able to compensate for the decreased insulin sensitivity, by increasing insulin secretion. However, ultimately, the pancreas does not manage to cope with the increased needs of insulin secretion, and impairment in glucose tolerance ensues. Even though this is the classical understanding of the pathophysiology of T2D, there is also evidence that hyperinsulinemia, per se, may also exacerbate insulin resistance (Del Prato et al., 1994). Furthermore, epidemiological evidence suggests that hyperinsulinemia, independently of insulin resistance, is an independent risk indicator of future T2D (Weyer et al., 2000).

2.2 Obesity, Type 2 Diabetes and Neurodegeneration

Alzheimer disease (AD) is the primary cause of dementia, accounting for two thirds of all dementia cases. Currently, there are more than 35 million patients affected with AD worldwide (Pugazhenthi et al., 2017).

Epidemiological studies have shown that obesity and T2D are risk factors for AD, and thus there are concerns that the incidence of AD could rise substantially in the following years, in line with the rise of obesity and T2D. A strong correlation between T2D and AD was first reported in the Rotterdam study, a large prospective study evaluating 6370 elderly subjects, which showed that patients with T2D have almost

double the risk of dementia and AD (Ott et al., 1999). It has also been shown that body mass index (BMI) is associated with reduced brain volume in patients affected by AD (Ho et al., 2010). A meta-analysis reported that obesity and T2D significantly and independently increased the risk for AD in elderly individuals (Profenno et al., 2010). However, in that study, the obese and patients with T2D had a smaller risk for developing AD than persons carrying the APOE4 allele, a gene that is linked to increased risk for AD (Michaelson 2014). T2D seems to affect women less favorably than men, since diabetic women over 65 years of age were found to have a higher rate of developing AD than elderly men with T2D (Wang et al., 2012).

Several studies have tried to evaluate the molecular links between AD and T2D. One suggestion has been the amylin receptor, as it is a target for both amylin and amyloid beta (Aβ) in the brain (Fu et al., 2013). Other studies have focused on the insulin effects on the brain, suggesting that decreased insulin action in the brain may have a role in the interplay between T2D and AD. More specifically, it has been shown that patients with AD have reduced expression and activation of the insulin receptor (IR), insulin-like growth factor 1 (IGF-1) receptor, and insulin receptor substrate 1 (IRS-1) proteins in the brain, and in the hippocampus and hypothalamus in particular (Steen et al. 2005). In line with this, in a small clinical trial it has been shown that intranasal insulin administration to patients with AD decreases the rates of cognitive dysfunction (Craft et al., 2012).

2.3 Brain Insulin Receptors

Insulin receptors and receptors of the IGF-1 are found throughout the brain. In the brain of mice, the insulin receptors are mainly expressed in the olfactory bulb, and to a lesser degree, in the cortex, the hippocampus, the hypothalamus, and the cerebellum (Zhao et al., 2004). In contrast, the IGF-1 receptor (IGF-1R) has the highest expression in the cortex, the hippocampus, and the thalamus, with only a moderate expression in the olfactory bulb, the hypothalamus, and the cerebellum (Fernandez and Torres-Aleman 2012).

In addition to topographic differences in their distribution, the two receptors, also have different physiological functions. Studies on mice with neuron-specific IR knockout (NIRKO) have shown that these animals have normal brain size and development, but exhibit clearly pathologic metabolic phenotypes, such as obesity and insulin resistance (Bruning et al., 2000). On the other hand, knockout of the IGF-1R in the brain results in reduced brain size, growth retardation, and behavioral changes (Kappeler et al., 2008).

Insulin levels in the cerebrospinal fluid are approximately 25% of those in the blood and increase proportionally after meals or with peripheral insulin infusion (Woods et al., 2003). Insulin enters the brain either via circumventricular regions

that lack a tight blood-brain barrier or through a receptor-mediated saturable transport system (Weindl and Sofroniew 1981).

Areas such as the hypothalamus, which lack an effective barrier, allow rapid access to insulin. Indeed, studies have shown that following peripheral insulin injection rapid activation of insulin signaling in these regions occurs (Kleinridders et al., 2013). Interestingly, in lower organisms, like Drosophila, insulin-like peptides are primarily produced by neurons (Fernandez and Torres-Aleman 2012). Even though, until recently, there was no evidence that insulin is produced in the brains of mammals, a study that has been very recently published suggests that in mice, insulin is produced in some restricted areas of the brain (Lee et al., 2020). The (patho)physiological significance of brain derived insulin is under study.

2.4 Central insulin effects on cognition, brain metabolism and whole-body homeostasis

Insulin has several functions in the central nervous system (CNS). The main behavioral actions of insulin in the CNS consist of regulation of cognition and feeding. In lean individuals, intranasal insulin increases the activity of memory-related areas (Kullmann et al., 2017; Marks et al., 2009).

Insulin in the brain also affects the control of body temperature. It has been shown that injection of insulin or IGF-1 into the preoptic area can activate brown adipose tissue and induce hyperthermia and that this effect is lost in the NIRKO mouse, indicating that it is mediated by the insulin receptor (Sanchez-Alavez et al., 2011). In humans, intranasal insulin administration has also been shown to enhance postprandial thermogenesis (Benedict et al., 2011).

Regarding brain metabolism, it has been long thought that insulin does not affect brain glucose utilization. However, in the beginning of the second millennium a [^{18}F]2-fluoro-2-deoxy-D-glucose ([^{18}F]FDG) PET study showed that BGU is decreased when somatostatin infusion is given compared to baseline, suggesting that insulin levels contribute to brain glucose metabolism in humans (Bingham et al., 2002). Later studies from our centre with the application of the euglycemic hyperinsulinemic clamp have shown that in the obese subjects and in subjects with impaired glucose tolerance (IGT), BGU is higher during the euglycemic hyperinsulinemic study than during the fasting state. Hence, when studying BGU during clamp, we have used the term “insulin-stimulated BGU”. Such an increase in BGU was not seen in the lean and normal glucose tolerant (NGT) subjects. It is important to note though that in both these studies, the groups of the lean and NGT subjects were small (N= 7 and 9, respectively), and thus it is unknown whether the effect of insulin on enhancing brain glucose uptake also in lean/NGT subjects was not seen merely because of lack of statistical power. In the same line, also in a PET

study in minipigs an effect of insulin on increasing BGU from the fasting state was seen in these animals, a phenomenon which, however, also did not reach statistical significance (Bahri et al., 2018).

One plausible explanation for the increased insulin-stimulated BGU in the obese subjects could be that this effect is driven by the higher circulating serum insulin typically seen in obese/insulin resistant subjects, because of decreased insulin clearance and higher insulin secretion. However, had this been the case, then the increased BGU should have been restricted in areas where the insulin sensitive glucose transporter GLUT4 is found and thus mainly restricted in the hypothalamus and the hippocampus (Williamson et al., 2012). However, the increases in BGU in the studies by Hirvonen *et al.* and Tuulari *et al.* are actually seen at the whole brain level, where mainly the insulin independent glucose transporters are present (GLUT1 in astrocytes, and GLUT3 in neurons). Moreover, the insulin transport through the blood-brain barrier (BBB) has been described to be a saturable process. The plasma-to-cerebrospinal fluid ratio of insulin has been described to be decreased in obesity (Kern et al., 2006). Still, the difference in BGU between obese and lean individuals is seen only during insulin stimulation, and not during the fasting state (Tuulari et al., 2013). Thus, clearly insulin plays a role, even though the mechanism is not yet understood.

At the whole-body level, animal studies suggest that in contrast to peripheral insulin, CNS insulin elevates blood glucose levels, decreases food intake and increases energy expenditure (Banks et al., 1997). In line with this NIRKO mice exhibit mild obesity and insulin resistance (Bruning et al., 2000). Direct central insulin action also affects serum insulin levels, even though the results are diverging. It has been reported that insulin given directly into the lateral hypothalamus stimulates parasympathetic outflow to the pancreas, while injection of insulin into the ventromedial hypothalamus has the opposite effect (Oomura and Kita 1981). Hypothalamic insulin signaling is also needed for insulin suppression of hepatic glucose production (Okamoto et al., 2005).

Recently it has also been shown that knock-out of the insulin receptor from astrocytes affects astroglial morphology (typically alterations in morphology are also followed by changes in function), reduces glucose sensing in specific hypothalamic neurons, alters systemic glucose homeostasis, and decreases BGU (Garcia-Caceres et al., 2016). Based on these findings the authors concluded that through insulin signaling astrocytes take part in CNS glucose sensing and that they are involved in controlling the systemic glucose metabolism (Garcia-Caceres et al., 2016).

2.5 Brain glucose metabolism and determinants of brain glucose uptake

The brain has a high demand of energy. Compared to the other organs, the brain consumes the highest amount of energy, which is approximately 20% of total body energy consumption, though it comprises only 2% of the typical human body mass (Mink et al., 1981). Most of the energy needed for the brain is used for sending and processing electrical signals across the brain's circuits. Probably as a consequence of this the neurons were considered to use most of the glucose that is taken up by the brain, while glial cells including astrocytes were considered to consume only a little of the glucose entering the brain. However, this notion has been challenged based on the findings of a preclinical PET study, where it was shown that the [^{18}F]FDG uptake in the brain was driven by astrocytes (Zimmer et al., 2017). This finding is in accord with what was originally proposed as the astrocyte neuron lactate shuttle (ANLS), whereby glutamate released by the neurons as neurotransmitter stimulates glucose uptake by astrocytes. Subsequently, astrocytes transform glucose into lactate, and provide lactate to the neurons (Pellerin and Magistretti 1994). However, this metabolic paradigm remains controversial (Diaz-Garcia et al., 2017).

In recent years, most *in vivo* human studies assessing brain metabolism have been performed either during the postabsorptive state or during insulin administration. The mode of insulin administration may also vary: either the euglycemic hyperinsulinemic clamp technique can be applied or insulin can be given intranasally. Pancreatic clamps where also somatostatin is infused to block endogenous pancreatic secretions have also been used. The application of intranasal administration of insulin has the advantage of providing high doses of insulin directly to the brain. Spillover, i.e. insulin going also in the systemic circulation is usually minimal. Using intranasal insulin administration, pioneering studies at Tubingen University have shown that intranasal insulin suppresses EGP in lean, but not in overweight individuals (Heni et al., 2017) (this study will be further discussed later).

We and other groups have addressed whether insulin resistance and T2D influence brain metabolic rates, assessed with [^{18}F]FDG-PET. However there is inconsistency in the yielded results. Several studies have reported that insulin resistance (assessed with HOMA-IR) and prediabetes/early-onset T2D associate with cerebral hypometabolism in key areas that are affected in AD (Baker et al., 2011). On the contrary, our group has previously shown that brain glucose uptake (BGU) during insulin clamp is higher in obese subjects and subjects with IGT compared to lean and NGT subjects, respectively (Hirvonen et al., 2011; Tuulari et al., 2013). Whereas differences during fasting BGU were not found between obese and lean subjects, the enhancement of BGU during insulin stimulation in obese and IGT subjects resulted in higher insulin-stimulated BGU in obese and IGT subjects than in lean and NGT subjects. Recently our group demonstrated that also subjects

with inherited insulin resistance (AKT-2 loss of function mutation, p.P50T/AKT2) had higher BGU during insulin-stimulation than age-matched controls (Latva-Rasku et al., 2017). This finding of increased brain glucose uptake in insulin resistance is "bizarre" if we consider that for instance in skeletal muscle obese subjects have lower glucose uptake than lean subjects in conditions of insulin stimulation. The molecular mechanism that is behind this "bizarre" characteristic of brain metabolism is thus far not understood.

Other important determinants of brain glucose uptake –when assessed during fasting- are age, and gender. It is agreed that brain glucose uptake decreases with aging. Goyal *et al.* conducted a meta-analysis of PET studies performed to quantify brain metabolic rates of glucose, oxygen extraction (cerebral metabolic rate for oxygen: CMRO2), and perfusion (Cerebral blood flow: CBF) (Goyal et al., 2017). For subjects over 45 years old, they reported median values of fasting BGU as ~22 μmol/100g/min, CMRO2 as~ 140 μmol/100g/min, and CBF as~ 44 mL/100g/min. The authors reported that with aging whereas brain glucose uptake decreases, brain oxygen extraction does not vary considerably. By coupling the glucose and oxygen extraction data, they concluded that this change in glucose metabolism with aging is largely due to loss of aerobic glycolysis, which represents the fraction of BGU that is not metabolized by oxidative phosphorylation (Goyal et al., 2017). Moreover, using PET imaging they further demonstrated that the regional topography of brain aerobic glycolysis changes significantly with normal aging.

There are also significant differences between the two genders. Several differences in brain structure and metabolic demands have been reported between men and women; these include differences in synaptic density (Alonso-Nanclares et al., 2008) and in neocortical thickness (Pakkenberg and Gundersen 1997). Several reports have also reported higher CBF in women compared to men. Recently, it has also been shown that whereas women have higher CBF in the cortical regions than men, the difference is lost in aging women suggesting, that a plausible mediator for the higher CBF in women of reproductive age is estrogen. Regarding brain metabolism, brain glucose utilization is not clearly different at the whole brain level. It is higher in female rats than male rats in specific brain areas, such as the hypothalamic medial preoptic area, the ventromedial nucleus, the median eminence, and the superior colliculus among a few others, but only when the female rats are studied during the premetestrous or metestrous period of the estrous cycle (Bishop and Simpkins 1992). Moreover, ovariectomy significantly decreases brain glucose utilization (Le Foll et al., 2009), whereas ovariectomized rats, which received estrogen replacement showed a 20-30% increase in brain glucose utilization in most brain regions. All in all, these data suggest that estrogens up regulate brain glucose utilization and that their effect is not restricted only to areas where sex steroid receptors are expressed (Bishop and Simpkins 1992; Namba and Sokoloff 1984).

2.6 Brain fatty acid handling

Lipids are an essential component of the brain both in terms of the structure of cellular membranes and in terms of the correct function of numerous cellular processes (Falomir-Lockhart et al., 2019). They make up approximately 50% of brain weight, which is the second highest lipid content after adipose tissue (Hamilton et al., 2007). It has been suggested that cerebral lipids are derived from both local synthesis and uptake from the blood (Rapoport et al., 2001). Once taken up by the BBB, neurons have fatty acid (FA) transporters. They also express enzymes for *de novo* lipid synthesis (Le Foll et al., 2009). However, astrocytes are the only brain cells able to oxidize FA, such as palmitate (further discussed in the chapter regarding astrocytes), whereas other FAs such as arachidonate, are mainly incorporated into phospholipids (Rapoport et al., 2001).

Cumulative evidence suggests that hypothalamic FA sensing regulates energy expenditure, insulin secretion and action, hepatic glucose production (HGP), and food intake (Cruciani-Guglielmacci et al., 2004; Lam et al., 2005; Obici et al., 2002a). For instance, prolonged intracerebroventricular (ICV) infusion of the long-chain fatty acid oleic acid decreases food intake as well as HGP (Obici et al., 2002b). It has also been shown that central FA infusion decreases the sympathetic tone (Magnan et al., 1999), which could contribute to the FA-induced increase of glucose-induced insulin secretion.

However, the physiological significance of such findings after direct ICV infusion can be questioned, since infusions of FA in the systemic circulation or directly into the carotid arteries are more physiological stimuli. Studies from Barry Levin's lab, using a microdialysis technique showed that after an 18-hour fast, high fat diet (HFD) leads to reduced caloric intake, with a delay of 3-6 hours. Moreover, by using hymeglusin, an inhibitor of astrocyte ketone production, they demonstrated that the effect was mediated through astrocyte ketone production, whereas the mechanism for this delayed effect on caloric intake was not addressed (Le Foll et al., 2014).

However, as discussed by the authors the concept that increases in brain FA levels acts as a satiety signal to inhibit feeding is contradictory to what one might expect since serum FFA are increased during fasting, a condition in which food intake should increase. Moreover, it is well established that early in the course of HFD, the hypothalamus becomes resistant to the adipostatic central actions of insulin and leptin (Prada et al., 2005). The induction of central leptin and insulin resistance has been suggested to be mediated through hypothalamic inflammation, and several potential mechanisms underlying hypothalamic inflammation in the context of HFD have been described (reviewed by (Velloso and Schwartz 2011)).

2.7 Astrocytes

Astrocytes (from the Greek words άστρο=star and κύτταρο=cell) are the most abundant type of glial cells, accounting for approximately 50% of all the brain cells (Verkhratsky A 2013). Astrocytes, along with the endothelial cells of brain capillaries and pericytes, form the blood-brain barrier. Moreover, in case of an ongoing inflammatory process, astrocytes become activated and proliferate (a term known as astrogliosis), in order to create a physical barrier between the inflammation and neurons, and thus restrict damage.

Because astrocytes are not electrically excitable, as neurons are, they have long been considered as only structural supporting cells for neurons. Against this until recently prevalent idea, astrocytes have received a lot of attention in recent years, and their importance in several aspects of not only energy homeostasis, but even evolution is currently under investigation.

Recent studies support the concept that astrocytes may have played a significant role in the evolution of higher cognitive function. For instance, it has been shown that while the rat cerebral cortex contains approximately 0.4 glia to neuron cells, the human brain has a ratio of approximately 1.4 (Friede 1954; Pelvig et al., 2008). In line with this, it is reported that when Albert Einstein's brain was examined the only difference that was found was that in the left cerebral area 39, Einstein's brain had a significantly low neuronal:glia ratio, when compared to the controls (Diamond et al., 1985). It should be noted, however, that this example is just an interesting anecdotal finding rather than conclusive proof that an increased glial number contributes to better cognitive function.

Regarding whole-body homeostasis there are several lines of evidence indicating direct and indirect control through astrocytes. First, hypothalamic astrocytes cooperate with specialized glucose sensitive neurons (Oomura et al., 1964) in detecting circulating glucose levels. This is suggested by studies showing that the expression of the insulin-independent glucose transporters GLUT1 and GLUT2 in astrocytes is critical for glucose sensing (Camandola 2018). Moreover, astrocytes are the only cell type in the brain able to utilize fatty acids either for oxidation (Edmond et al., 1987) or for the synthesis of ketone bodies (Edmond 1992). Furthermore, astrocytes express receptors for most of the hormones involved in energy homeostasis, including leptin (Diano et al. 1998), ghrelin (Fuente-Martin et al., 2016), IGF-1 (Garcia-Segura et al., 2000), thyroid hormone (Dezonne et al., 2015), glucagon like peptide-1 (GLP-1) (Reiner et al., 2016), and insulin (Garcia-Caceres et al., 2016).

Another interesting characteristic regarding astrocytes is that astrocytes in females and in males exhibit marked structural differences that could account, at least to some degree, for the gender specific differences in energy homeostasis. First, a female's astrocytes have a simple bipolar structure compared to the complex stellate shape found in males (Mong et al., 1999). Second, they express receptors for estrogen, androgen and progesterone, which could explain the morphological

changes and possible different functional responses of hypothalamic astrocytes between males and females (Chowen et al., 2018; Garcia-Ovejero et al., 2005). Glial structural changes are seen in the hypothalamic areas both in rodents and in humans during the estrous cycle (Baroncini et al., 2010). It has also been shown that following HFD hypothalamic inflammation and astrogliosis is worse in male rodents than females. The combination of the above indicates that astrocytes are instrumental in regulating the responses of males and females to overfeeding.

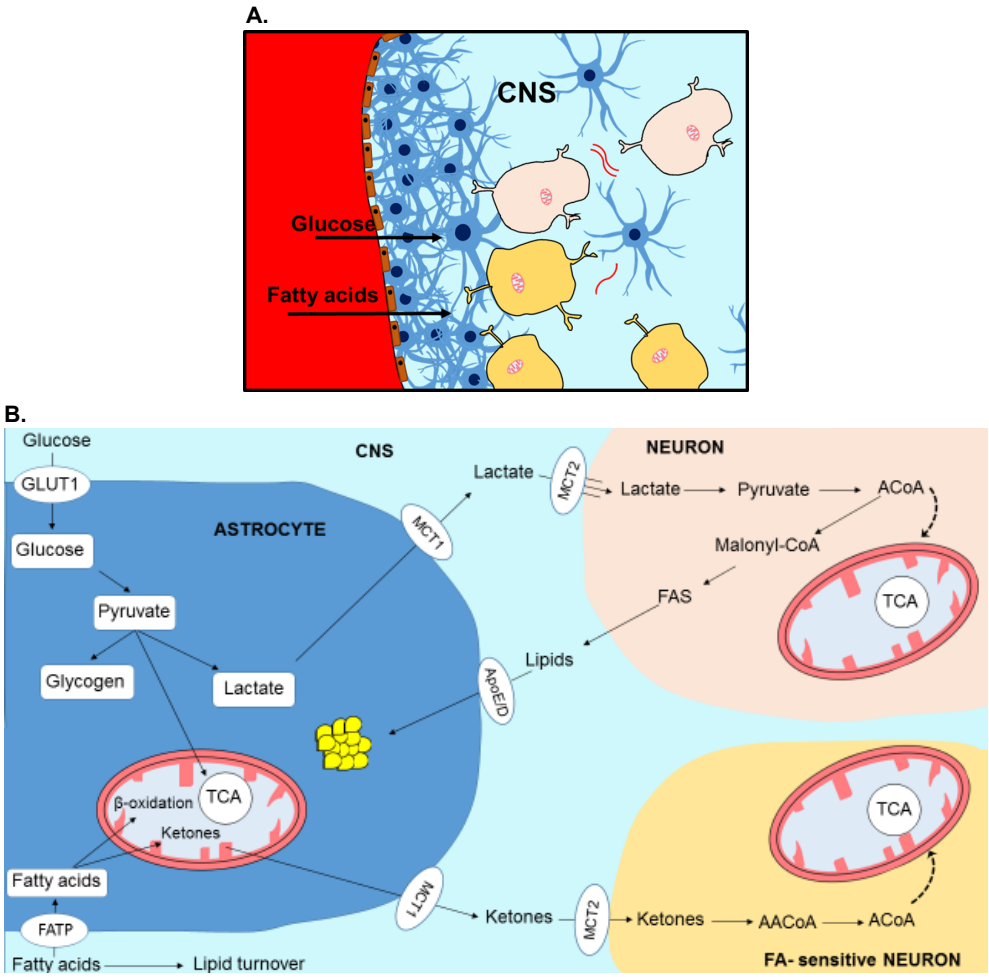

Figure 1. Astrocytes are the energy hubs of the brain. They take up glucose and convert it to lactate through the astrocyte neuron lactate shuttle (ANLS). The fatty acids that are taken up by astrocytes can be oxidized, or used for ketone production. Brain glycogen is also exclusively found in astrocytes. **A**) Astrocytes (along with brain endothelium, and pericytes) form the BBB. **B**) Zoomed image of **A)** to show the metabolic pathways between astrocytes and neurons (Exemplified Figures). FAS: fatty-acid synthesis; ACoA: acetyl-CoA; AACoA: acetoacetyl-CoA; MCT: monocarboxylate transporters; FATP: fatty-acid transporter.

2.8 Central inflammation and astrogliosis in obesity

Astrocytes are the most abundant glial cells of the CNS and are characterized by numerous cytoplasmic processes radiating from the glial cell body or soma. All astrocytic processes contain intermediate filaments of glial fibrillary acidic protein (GFAP), and antibodies against this protein provide a simple method to stain these cells. Astrocytes form part of the BBB and help regulate the entry of molecules and ions from blood into CNS tissue. Although the association between obesity and low-grade systemic inflammation is well established in humans (Hotamisligil 2006), evidence of obesity-related cerebral inflammation in humans is still lacking.

Preclinical studies have shown that overfeeding with HFD induces astrocyte proliferation in rats, a term known as astrogliosis (Thaler et al., 2012). Interestingly, hypothalamic inflammation develops within few days from the onset of HFD, before significant weight gain occurs, and it is concomitant with the onset of leptin resistance and upregulation of neuronal stress factors (Munzberg et al., 2004; Thaler et al., 2012). In line with this, it has been shown that genetically modified mouse models with decreased inflammatory signaling (mice deficient in the toll-like receptor adaptor molecule MyD88), were protected from the HFD-induced weight gain and from the development of leptin resistance (Kleinridders et al., 2009)

Furthermore, Thaler and colleagues provided evidence of astrogliosis in human obesity by showing a positive association between BMI and the hyperintensity of the mediobasal hypothalamus (MBH) compared to the amygdala assessed by MRI (Thaler et al., 2012). This finding was later confirmed also by applying a quantitative MRI technique to measure relaxation time in the MBH, with both obesity and insulin resistance being associated with higher MBH intensity and, therefore hypothalamic gliosis (Schur et al., 2015).

It has also been recently shown that the signal from [^{18}F]FDG-PET in the brain is more likely driven by astrocytes and not by neurons as originally thought (Zimmer et al., 2017). Thus, central inflammation and astrogliosis could offer a plausible explanation for the increased insulin-stimulated brain glucose uptake in obese and insulin resistant subjects seen consistently in our previous studies (Hirvonen et al., 2011; Tuulari et al., 2013). This hypothesis is currently under investigation by our group, but is not included in the present thesis.

2.9 Methods to measure brain substrate metabolism in humans

2.9.1 Arteriovenous difference technique

Arteriovenous difference (AV) technique is based on the concentration difference of a metabolite between an artery delivering the tissue of interest and a vein leaving from the tissue (Zierler 1961). By applying this method Owen and colleagues have shown that during fasting the brain extracts glucose and ketone bodies (Owen et al., 1967). A subsequent study showed that, in the postabsorptive state, during euglycemic hyperinsulinemia, as well as during hypoglycemia, glucose is the main substrate for oxidation in the brain. Moreover, in the first two conditions (postabsorptive state and euglycemic hyperinsulinemia), glucose uptake could account for practically the entire oxygen consumption. During acute hypoglycemia, glucose could account for approximately 90-92% of oxygen consumption, indicating that other substrates are also used (even though still in small amounts) by the brain (Wahren et al., 1999). As this technique is highly invasive, its use has been limited in recent years.

2.9.2 Magnetic resonance spectroscopy

With magnetic resonance spectroscopy (MRS), also known as nuclear magnetic resonance (NMR) it is possible to measure concentrations of various metabolites inside the tissue of interest. Thus, compared to AV differences technique and positron emission tomography, MRS has the advantage of not being invasive and not exposing the participants to ionizing radiation. Regarding the physics of MRS, MRS is feasible "on any nucleus possessing a magnetic moment" (de Graaf 2018). The most commonly used nuclei with this property are proton (^{1}H), carbon-13 (^{13}C), phosphorus (^{31}P) and sodium (^{23}Na). Even though the number of relevant nuclei is limited, MRS provides the unique possibility to study simultaneously several metabolites. Thus, ^{1}H MRS, using the proton nucleus, which is the most sensitive nucleus for MRS, allows the detection of a number of important neurotransmitters, such as glutamate and GABA, other metabolites, such as N-acetyl-aspartate, creatine, glutamine, and choline as well as glucose and lactate.

With ^{13}C MRS it is possible to study the fluxes through important metabolic pathways, like the Krebs cycle. Also glycogen deposits can be studied with ^{13}C MRS. ^{31}P MRS provides information about energetically important metabolites, such as ATP, intracellular pH, and reaction fluxes (de Graaf 2018).

The application of MRS techniques in the clinic is potentially interesting. However, MRS is challenging for several reasons. First and foremost, because of the

magnitude of water resonance (which is much larger than the concentration of the metabolites), the detection of metabolites of interest can be difficult. Secondly, other large signals such as extracranial lipids, can also interfere with small metabolite signals. Thirdly, heterogeneous magnetic field distributions significantly decrease the spectral resolution (de Graaf 2018).

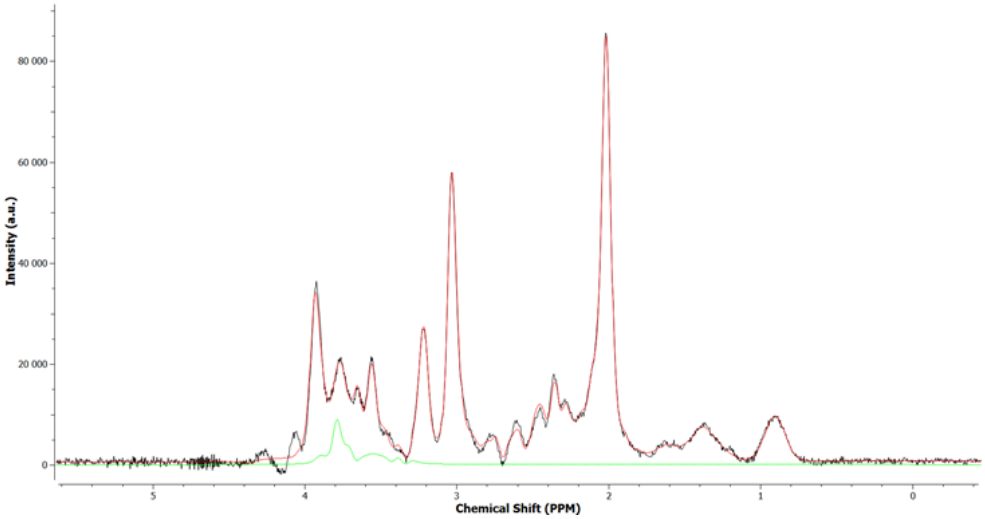

Figure 2. A typical ^{1}H NMR spectrum acquired from an obese volunteer (source: BARIBRAIN study). The green line shows the glucose peak. The red line shows the ''raw'' acquired spectrum.

2.9.3 Positron emission tomography

Positron emission tomography (PET) is a medical imaging technique, which utilizes short half-lived radionuclides incorporated into biological molecules, in order to image molecular processes. Nowadays PET is considered the gold standard technique for measuring substrate turnover in humans *in vivo*. The positron emitting radionuclides are produced with a cyclotron. The most common way of administrating a radiotracer is intravenously, but also other modes of administration can be used; for instance, the inhalation of gaseous tracers like marked oxygen [^{15}O]O_2 and marked carbon dioxide [^{15}O]CO_2 (Turku and Oikonen 2019). The tracers are usually administered in bolus by the researcher in charge, but in case of very short-lived tracers (like radiowater), automated systems are used for the administration of the tracer. A PET scanner detects the radioactivity of the tracer that accumulates in the tissues of interest. The acquired data are then transformed into an image, which is analyzed using adequate modeling. Depending on the tracer used and the modeling that will be applied for the analysis of the data, blood samples

(arterial or "arterialized" venous) are taken for measuring radioactivity in plasma and the proportion of metabolites.

Figure 3. The study volunteer is lying inside the PET/CT scanner (GE Discovery,"*Sampo*"), with only the covered legs in view. The researcher is performing a euglycemic clamp in combination with PET scanning. Depending on the organ/tissues studied the volunteer enters a specific depth inside the PET camera. Notice also the two infusion lines for glucose and insulin. Rhythm of ECG is also monitored during the whole length of the study. Photo taken by Sanna Himanen. In the PET Centre, it is common to name the PET scanners based on names from the Finnish early 19th-century national epic story of *Kalevala.* Other names for PET scanners currently in use are "*Aino"* and *"Ilmari"*.

2.10 Physical principles of the PET

By definition, PET tracers emit positrons, and thus the tracer undergoes nuclear decay continuously. The emitted positrons collide with electrons and, as a result, are annihilated. The process of annihilation converts the mass of these colliding particles into energy and consequently two gamma (γ) photons of equal energy are emitted in opposite directions. The emitted gamma photons are detected by the PET scanner. The obtained raw data is processed by computers to form a reconstructed tomographic image.

Most of the photons are however lost because of their absorption into the body, the amount depending on the size of the body in the field of view.

This loss of detection is called attenuation. Attenuation varies depending on the studied organ (for instance attenuation is low in the lungs, and high in dense tissues such as bones) (Turku and Oikonen 2019). Attenuation leads to severe artefacts in the PET image, and attenuation correction is warranted during image reconstruction. This is the main reason why low resolution CT images are also acquired (for the attenuation correction) when PET studies are performed.

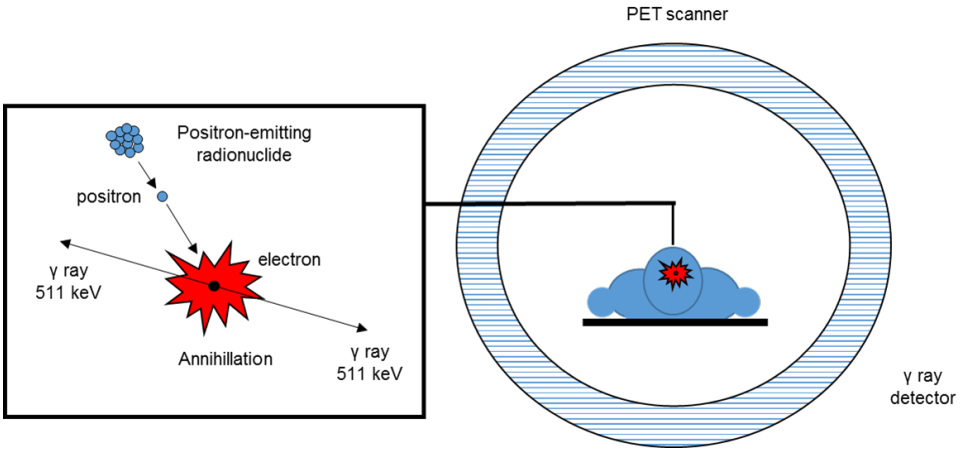

Figure 4. Drawing depicting the principles of PET; Modified from van der Veldt et al., 2013.

The two tracers that have been used in this thesis are [^{18}F]FDG and 14(R,S)-[^{18}F]fluoro-6-thia-heptadecanoic acid [^{18}F]FTHA.

2.11 Limitations of PET Imaging

Administration of a PET tracer causes exposure to ionizing radiation for the studied subject. For this reason, the number of studies that can be performed on one study volunteer is limited. For instance, a typical dose for brain (and rest of the body) during [^{18}F]FDG imaging of 180 MBq of [^{18}F]FDG corresponds to an effective dose of 3.5 mSv, whereas the mean annual background radiation dose in Finland is 3.2 mSv. The radiation from computerized tomography, taken for the attenuation correction should also be added to this amount of ionizing radiation burden. The effects of such a dose on the subject's health are marginal. However, there are ethical guidelines, which set the maximum acceptable radiation burden for healthy individuals in order to ensure safety. Typically this radiation limit is around 10 mSv. PET imaging cannot investigate more than one function at a time. Thus, if the [^{18}F]FDG tracer is given, only glucose uptake can be evaluated, whereas if [^{18}F]FTHA is given, free-fatty acid uptake can be addressed. In case more than one

function is to be studied (for instance both perfusion and glucose uptake), the necessary time for complete decay of the first tracer needs to have passed before administering the second tracer. This can make PET studies especially time-consuming. The field of view of the PET scanner also limits the ability to study several organs. Furthermore, the resolution of the (current) PET scanners is about 3.5 mm, which limits the possibility to study very small brain areas, such as the hypothalamus.

2.12 Bariatric surgery as a treatment for morbid obesity

Diet modification, and lifestyle intervention have proved to be only a weak arm in the battle against obesity. Even though considerable weight loss can be achieved with lifestyle interventions (up to 20% of initial body weight) (Weiss et al., 2007), when the lifestyle intervention is stopped, weight regain typically occurs. Moreover, some studies have shown that the higher the weight loss during the lifestyle intervention, the higher the weight regain once the intervention is ceased (Weiss et al., 2007). Weight regain can be detrimental since weight cycling may have adverse health effects (Vergnaud et al., 2008), and even lead to increased all-cause mortality and mortality from coronary disease (Brownell and Rodin 1994). In contrast, bariatric surgery (BS) is the most powerful weapon in the battle against morbid obesity. Apart from inducing rapid weight loss, it is also very effective in maintaining weight loss, with an average of 32 kg weight reduction at five years after intervention (Puzziferri et al., 2014).

Before surgery, candidates for BS, undergo thorough screening to exclude primary causes of obesity and other disorders which could jeopardize the weight loss achieved after bariatric surgery, or even risk the patients' health. Subjects also receive nutritional counseling by a dedicated nutritionist. Before surgery, subjects undergo a very-low calorie diet, during which they must lose weight. Weight loss prior to surgery is a fundamental prerequisite and is also an additional safety measure, since it helps in the surgical procedure. Even though several bariatric surgery types have been described the most successful ones worldwide are: 1) Roux-en-y gastric bypass, which is a combination of restrictive and malabsorptive intervention and 2) Sleeve gastrectomy (usually performed laparoscopically, so the abbreviation commonly used is LSG), which is purely restrictive.

Although BS has numerous beneficial effects, including remission of T2D, it can also have serious and life-threatening adverse effects. Among these, postprandial hypoglycemia (PPHG) is a common, but often under-diagnosed complication of both RYGB and LSG (Seaquist et al., 2013). Also, some degree of weight regain typically occurs one to two years after surgery, and it has been recently shown that subjects

suffering from postprandial hypoglycemia lose less weight compared to those who do not develop post prandial hypoglycemia (Rebelos et al., 2020a). Subjects who have undergone RYGB or other malabsorptive treatments (for instance biliopancreatic diversion) also risk vitamin, and ferrum deficiencies and thus, long (even lifelong) follow-up is needed. All in all, BS is today the most powerful method to achieve weight loss and improvement of the glucometabolic status in subjects affected by morbid obesity. However, it is also a treatment that follows the subject for his/her whole life-time, so special attention need to be paid to the selection of good candidates for undergoing BS. Additionally, frequent medical controls are warranted in order to achieve the best outcomes and minimize adverse events related to BS.

For the aims of the studies enclosed in this thesis, which focused on the effects of obesity and weight loss, BS provides an excellent interventional approach.

3 Aims

This thesis set out to investigate whether the brain (through brain substrate handling) is involved in the control of whole-body homeostasis and whether an increased brain substrate uptake predicts any metabolic outcome at follow-up.

The specific objectives of this thesis are:

I. To evaluate whether brain glucose uptake correlates with endogenous glucose production in morbidly obese and lean subjects and whether bariatric surgery affects such potential association.
II. To evaluate whether brain substrate utilization correlates with the parameters of beta cell function assessed with oral glucose tolerance modeling.
III. To evaluate whether brain fatty acid uptake is higher in morbidly obese than lean women and whether brain fatty acid uptake is decreased following bariatric surgery.

4 Materials and Methods

4.1 Study subjects

This thesis includes data from a total of 124 subjects, who each participated in one of the three studies presented. All study participants were Caucasian. None of the study subjects had any clinical diagnoses of neurological diseases or severe psychiatric disorders. All subjects underwent a screening visit before inclusion in the study. Prior to inclusion, each participant gave written informed consent. Each study protocol included in this study was approved by the Ethics Committee of the Hospital District of Southwest Finland and conducted in accordance with the Declaration of Helsinki.

Study I included 20 morbidly obese subjects eligible for BS and 14 lean controls. Of the 20 obese subjects, 17 returned for the post-bariatric surgery studies. In study II cross-sectional data of 120 subjects were included. Study III consisted of 24 morbidly obese subjects and 14 lean individuals. 21 obese subjects were re-studied after BS. Of note, the study participants in study I and III were included in the cross-sectional dataset of study II.

Inclusion criteria for the patient population

1) BMI > 40 kg/m^2 or > 35 if there is an additional risk factor (for instance T2D, sleep apnea)
2) Age: 18-60 years
3) Previous, carefully planned, conservative treatments for obesity have failed

Exclusion criteria for the patient population

1) BMI > 60 kg/m^2
2) Weight more than 170 kg
3) Waist circumference > 150 cm
4) Mental disorders or poor compliance
5) Eating disorders (e.g. binge eating) or excessive consumption of alcohol

6) Active peptic ulcer disease
7) T2D requiring insulin treatment or fasting glucose more than 7 mmol/l

Inclusion criteria for the control group

1) BMI 18-27 kg/m^2
2) Age 18-60 years
3) Fasting plasma glucose < 6.1 mmol/l
4) Normal glucose tolerance test (studied with OGTT)

Exclusion criteria for healthy participants

1) Blood pressure > 140/90 mmHg
2) Mental disorder or poor compliance
3) Any chronic medical defect or injury which hinders/interferes with everyday life
4) Eating disorder or excessive use of alcohol

Exclusion criteria for both groups

1) Pregnancy
2) Past participation in nuclear medicine imaging studies
3) Any other condition that in the opinion of the investigator could create a hazard to subject safety, endanger the study procedures, or interfere with the interpretation of study results
4) Presence of any ferromagnetic objects that would make magnetic resonance imaging contraindicated

Table 1. Characteristics of the study participants*.

Study	Characteristics	Number of subjects	Age (years)	Sex (M/F)	BMI ($kg \cdot m^{-2}$)	PET tracer(s)	Scanning conditions
I	Obese before and after BS and lean controls	20 obese and 14 lean	47 ± 8	5/29	37 ± 10	[^{18}F] FDG	Euglycemic clamp and Fasting
II	Cross-sectional data of all subjects who had β-cell function data and PET	67 study (a), 34 study (b), 45 study (c)	46 ± 9, 45 ± 9, 43 ± 11	13/54, 0/34, 10/35	32 ± 9, 34 ± 10, 34 ± 10	[^{18}F] FDG [^{18}F]FTHA	Euglycemic clamp and Fasting
III	Obese before and after BS and lean controls	24 obese and 14 lean	43 ± 11	(0/38)	34 ± 10	[^{18}F]FTHA	Fasting

* In Study II (a): 67 subjects studied with [^{18}F]FDG under euglycemic hyperinsulinemic clamp; (b): 34 women studied with [^{18}F]FTHA under fasting conditions; and (c): 45 subjects studied with [^{18}F]FDG during fasting.

4.2 PET-studies (I-III)

Insulin clamp [^{18}F]FDG studies (I, II): The euglycemic hyperinsulinemic clamp was performed as previously described (DeFronzo et al. 1979). In brief, after an overnight fast, the subjects were given a primed-continuous infusion (40 mU·m^{-2}·min^{-1}) of insulin (Actrapid; Novo Nordisk, Copenhagen, Denmark). During the clamp, a variable rate of a 20% glucose solution was infused in order to maintain euglycemia (5 mmol/L). Plasma glucose levels were measured every 5–10 minutes throughout the study. Approximately 100±10 minutes into the clamp, [^{18}F]FDG (187±9 MBq) was injected intravenously over a 15 second period and brain [^{18}F]FDG radioactivity was measured either immediately thereafter for 40 minutes (dynamic scan) or after 70–80 minutes (static scan for 10 minutes). For this reason, when studies were pooled and re-analyzed (as in study II) the time interval between the [^{18}F]FDG injection and the brain scan was also used as a covariate in the statistical analysis. During the clamp, plasma glucose, plasma insulin and serum FFA were taken at baseline and every 5, 30 and 60 minutes respectively. The M-value (the index of insulin sensitivity, from "Metabolised glucose") was calculated by using three 20 minutes time intervals, between 60 and 120 minutes into the clamp.
Fasting [^{18}F]FDG studies (I, II): During fasting, an intravenous bolus (188±7 MBq) of [^{18}F]FDG was given, following which the dynamic PET imaging of the brain started and continued for 40 minutes. Blood samples were drawn periodically during the entire scanning period to measure radioactivity levels.

[^{18}F]FTHA studies (II, III): Following an overnight (10–12 h) fast, an intravenous bolus (185±46 MBq) of [^{18}F]FTHA was given, following which the dynamic PET imaging of the brain started and continued for 40 minutes. Blood samples were drawn during the entire scanning period to measure FFA as well as radioactivity levels and metabolites.

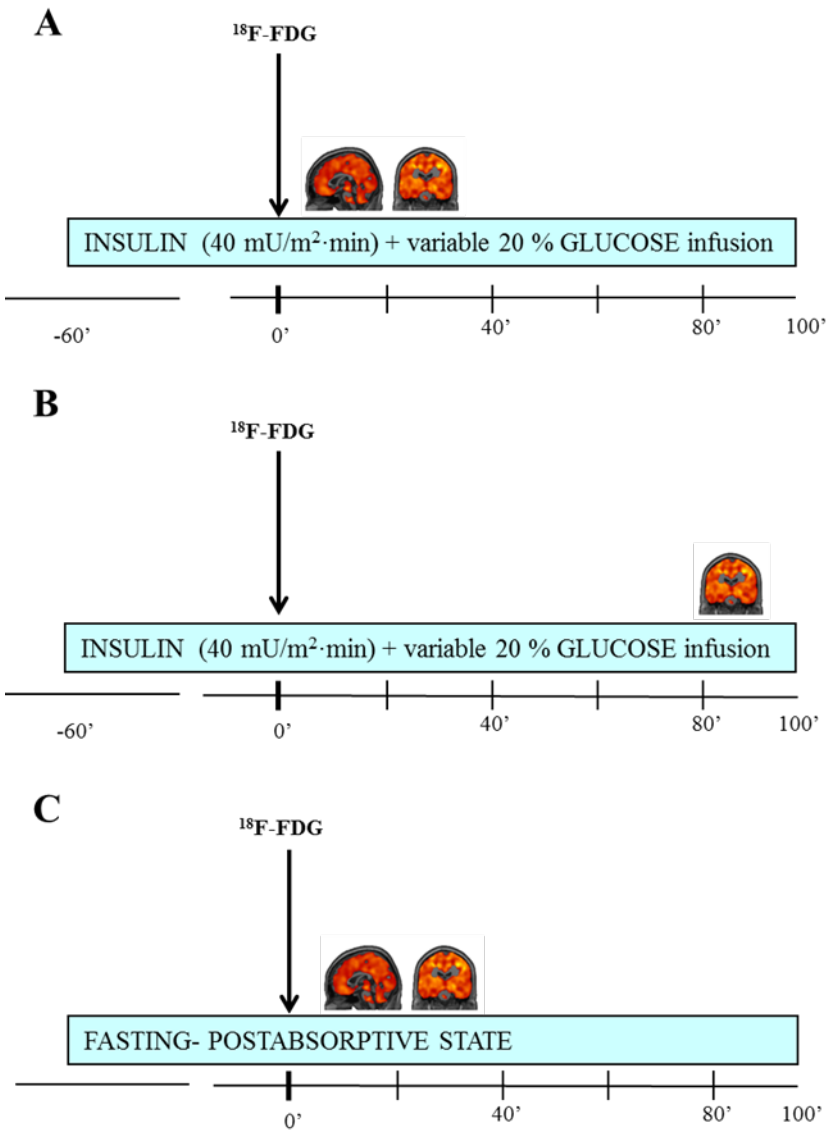

Figure 5. Diagram of the experimental protocol of the [^{18}F]FDG-PET studies during euglycemic hyperinsulinemic clamp (A, B) and fasting (C). The difference between studies (A) and (B) is that in (A) brain radioactivity is acquired immediately after [^{18}F]FDG injection and lasts for 40 minutes, whereas in (B) brain radioactivity is acquired at the end and lasts for only 10 minutes.

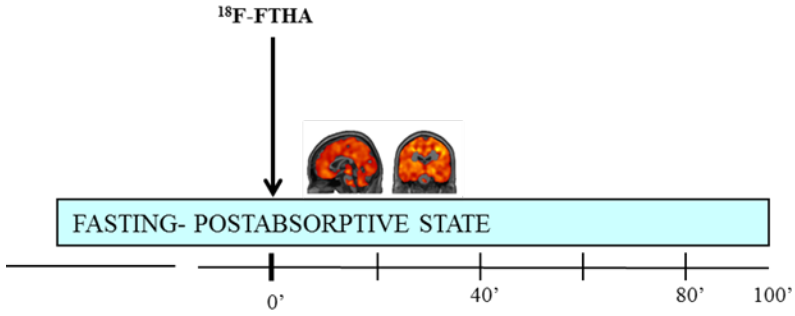

Figure 6. Diagram of the experimental protocol of the [^{18}F]FTHA-PET. Studies were performed in the postabsorptive state. Note that the fasting [^{18}F]FDG-PET and [^{18}F]FTHA-PET protocols are identical. Brain radioactivity was acquired immediately after [^{18}F]FTHA injection, and lasted for 40 minutes.

4.3 Production and characteristics of radiotracers (I-III)

The glucose analogue [^{18}F]FDG ($T_{1/2}$ =110 min) was produced with an automatic apparatus by a modified Hamacher method (Hamacher et al., 1986). After entering the cells, [^{18}F]FDG is phosphorylized and remains trapped in tissue in proportion to its phosphorylation rate.

The palmitate analogue [^{18}F]FTHA ($T_{1/2}$ =110 min) was synthesized by labelling 14(R,S)tosyloxy6-thia-heptadecanoic acid with [^{18}F]fluoride and with high-performance liquid chromatography (Takala et al., 2002). After entering the cell, [^{18}F]FTHA goes through partial mitochondrial β-oxidation, and remains trapped (Iozzo et al. 2003). In contrast to the other palmitate analogue available (^{11}C-palmitate), [^{18}F]FTHA shows total fatty acid uptake, whereas ^{11}C-palmitate undergoes rapid β-oxidation and the remaining radioactivity represents the non-oxidized part (Karmi et al., 2010).

The information regarding the fate of [^{18}F]FDG and [^{18}F]FTHA after entering the cells is exemplified and presented in **Figure 7**.

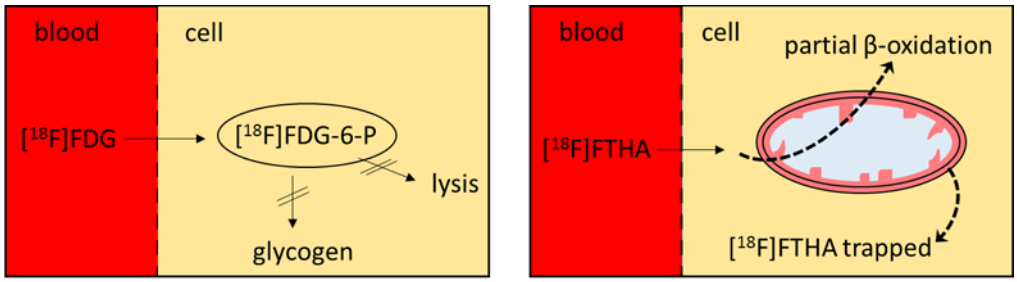

Figure 7. Exemplified cartoon depicting what happens when [^{18}F]FDG and [^{18}F]FTHA enter the cells.

4.4 PET scanners, PET image acquisition and data processing

The studies were performed using either the GE Advance PET camera (General Electric Medical Systems, Milwaukee, WI), GE Discovery STE (General Electric Medical Systems, Milwaukee, WI, USA), or ECAT931/08 (Siemens Molecular Imaging, Inc., Knoxville, TN, USA). The scanners were cross-calibrated against the same VDC-404 Dose calibrator (COMECER Netherlands, Joure, the Netherlands). All data were decay- and attenuation- corrected, and reconstructed using a Hann filter with a cut-off frequency of 0.5 and a median root prior to reconstruction method 3. Blood samples from an "arterialized" vein were drawn during the study and analyzed for radioactivity concentration in plasma using an automatic γ counter (Wizard 1480, Wallac, Turku, Finland), and measurement of radioactive metabolites (applicable for [^{18}F]FTHA studies) .

All studies were pre-processed similarly via the internally developed pipeline named MAGIA (http://emotion.utu.fi/softwaredata/) (Karjalainen et al. 2020). Dynamic PET images were motion corrected and mean images were calculated. Mean PET images were spatially normalized to the [^{18}F]FDG template in Montreal Neurological Institute (MNI) space (MNI International Consortium for Brain Mapping) using SPM12 (www.fil.ion.ucl.ac.uk/spm/) running on Matlab for Linux (version 9.1.0; Math Works, Natick, MA). Normalization parameters were subsequently applied to corresponding dynamic images and Ki (influx constant rate) parametric images were calculated. Parametric images were smoothed at 8 mm full-width at half-maximum.

A global and eight other brain regions of interest (CER-A, anterior cerebellum; CER-P, posterior cerebellum; FRO, frontal lobe; LIMB, limbic lobe; MID, midbrain; OCC, occipital lobe; PAR, parietal lobe; TEMP, temporal lobe) were selected via wfu pickatlas (www.fmri.wfubmc.edu/cms/software) and extracted from the parametric images via Marsbar (in order to perform the linear regressions with the various predictors).

4.5 PET imaging

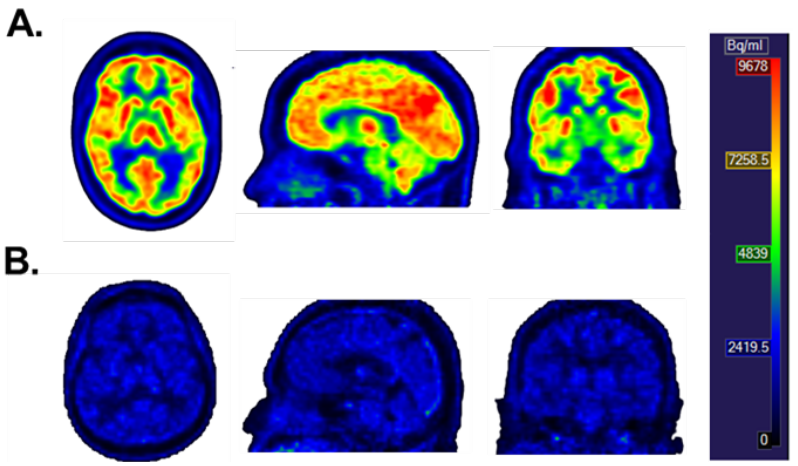

Figure 8. Raw [^{18}F]FDG-PET and [^{18}F]FTHA-PET mean images presented on the same scale, to show visually to the reader the obvious differences in brain glucose uptake and brain fatty acid uptake. Even though the brains of different subjects are illustrated, subjects were matched for sex (women), age (42 years), and BMI (40 kg·m^{-2}).

4.5.1 PET Quantification: semiquantitative and quantitative approaches

There are several approaches to presenting PET data. Generally, these are divided into the semiquantitative and quantitative approaches.

Standardized uptake value (SUV) is a semiquantitative method for assessing tissue metabolic uptakes, which are calculated by dividing tissue radioactivity concentration by injected dose and multiplied by body weight (SUV=radioactivity concentration/(dose/body weight)) (Turku and Oikonen 2019). In principle, SUV is based on the fact that the administered dose divided by the subject's body weight represents the mean radioactivity concentration in the whole body, and that the average SUV in one person (whole body) is 1 g/ml. For example, if there is increased/decreased uptake in some tissue (for instance, adipose tissue), it will affect the SUV in the region of interest (for instance, brain), even though this is not due to the characteristics of the tissue of interest, but rather, it depends on the availability of the tracer. Accuracy of SUV is inferior to the quantitative three-compartment modeling, Patlak plot and fractional uptake rate (FUR), which account for the (variability of the) availability of the tracer in arterial plasma.

For quantitative approaches blood sampling (or acquisition of aorta images within the field of view) is mandatory in order to account for the input curve. Full compartmental model is the gold standard for quantitative PET analysis. It requires

radioactivity acquisition from the start of the study (injection of the tracer), and frequent sampling. Full compartmental model is however usually not used because both graphical analysis (Gjedde-Patlak plot) and FUR represent reliable alternatives.

In the Gjedde-Patlak plot, plasma input data must be collected from the injection of the tracer. Tissue (of interest) data can be either acquired either immediately after injection of the tracer or later. Typically, when tissue data are acquired immediately after injection, the first 15-20 minutes are excluded from the analysis, in order to obtain a stabilization period of the tracer in the examined tissue. This discarding of the first minutes of the tissue data, is mandatory so that when the Gjedde-Patlak plot is applied, equilibrium of the tracer (in the extracellular and intracellular compartments) of the tissues is achieved, and thus the plot becomes linear. This is better explained in the Figures that follow. **Figure 9A1** shows the plasma and tissue curves of [^{18}F]FDG from injection until 40 minutes of scanning. The time frame from 20 minutes until the end of the scan is selected to be analysed. When applying the Gjedde-Patlak plot (**Figure 9A2**) a line is created, where at the y axis there is tissue concentration/plasma concentration, and at the x axis there is the area under the curve (AUC) of tissue concentration/plasma concentration. The slope of the line represents the influx constant (Ki) which is then multiplied by the circulating substrate levels (for [^{18}F]FDG, with plasma glucose), and this value represents the tissue glucose uptake. In case of [^{18}F]FDG a lumped constant correction is also applied to account for the difference between glucose and [^{18}F]FDG uptake from the studied tissue.

Also, whereas FUR tissue data can be acquired immediately after injection, or in a later phase, plasma input data must be available from injection. When FUR is applied the radioactivity value of the middle of the selected frame used is divided by the integral of plasma input curve from the beginning until the same time point that was used for the tissue radioactivity (**Figure 9B**). Then, the same procedure as described above for the Gjedde-Patlak plot is performed in order to obtain glucose (or fatty acid) uptake values.

Results from Gjedde-Patlak plot and FUR analysis show excellent correlation.

A1.

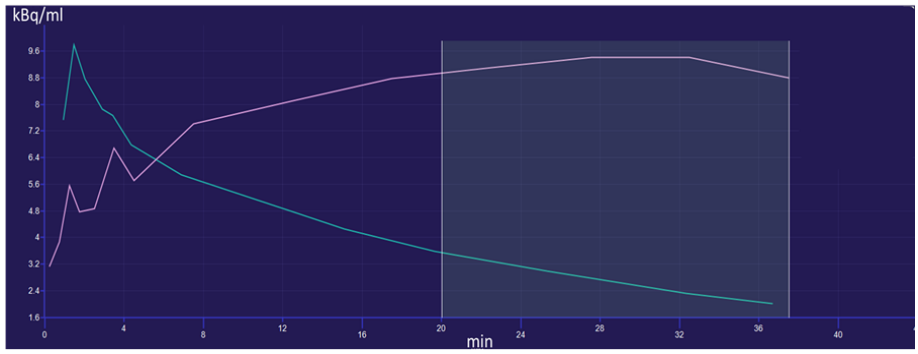

A2.

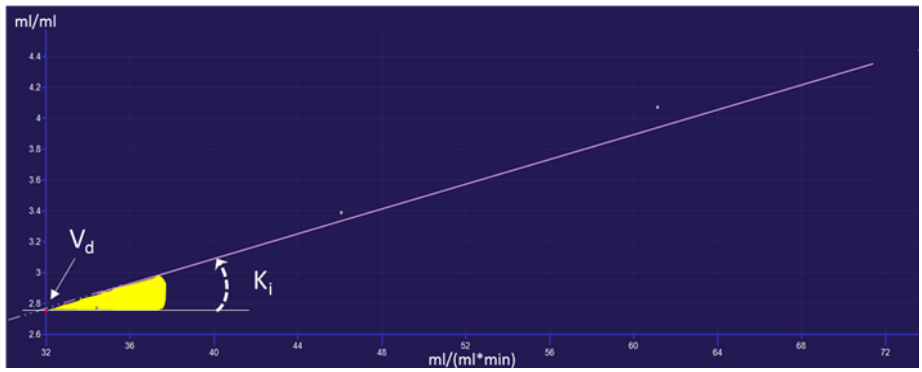

B.

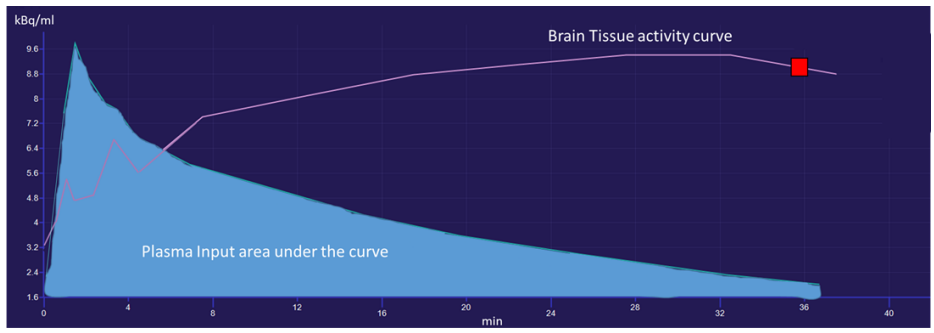

Figure 9. **A1** and **9A2** figures showing the principle of the Gjedde-Patlak plot. First, the time range is selected (in this case from 20 min to the end of the brain scan). Blue line shows plasma input curve, and purple line shows the brain tissue activity curve. Then, when the Patlak plot is applied, the model gives the volume of distribution (Vd) that is the point where the modelled tissue curve crosses the Y axis (intercept). The slope of this line (showed in yellow), gives the Ki. Glucose uptake can then be calculated as Ki multiplied by the average plasma glucose levels from the injection of [^{18}F]FDG to the middle of the scan, and divided by the lumped constant (GU= Ki*PG/LC). **B** figure showing how glucose uptake can be calculated with FUR calculation. FUR =tissue radioactivity at the selected time point (in this case the middle point of the frame from 30-40 min) divided by the integral of plasma input curve from the beginning until the same time point that was used for the tissue radioactivity. To obtain GU values FUR is then multiplied by the average plasma glucose levels from the injection of [^{18}F]FDG to the middle of the scan.

4.5.2 Modeling

In study (I), brain glucose uptake was quantified from [^{18}F]FDG by using graphical analysis to calculate the influx constant rate of tracer uptake (Ki) (Patlak and Blasberg 1985). The input function for graphical analysis was derived from arterialized blood samples. The rate of glucose uptake (micromoles per gram per minute) was calculated by multiplying Ki by the plasma glucose concentration (from [^{18}F]FDG injection to the end of the brain scan) and dividing this by the lumped constant of the brain, and the brain density (1.04 g/ml).

In study (II), a different approach was used since studies where brain radioactivities were acquired at different time points were pooled together. Brain glucose uptake was quantified using FUR. This variation was needed because, for early studies graphical analysis, and FUR were possible options, but for the late studies (since brain radioactivity was static at the late studies), the slope of the line could not be determined and as such, FUR was preferable.

For all [^{18}F]FDG-PET studies the lumped constant value for the brain was set at 0.65 (Wu et al. 2003).

In studies (II, and III), fatty acid uptake was simply quantified using FUR as BFAU = FUR*(fatty acids).

4.6 Endogenous glucose production (EGP) determination (I)

EGP was calculated, as previously described, by Iozzo *et al.* (Iozzo et al. 2006). Of note, this method has been validated against the gold standard of D-[6,6-^{2}H] glucose.

In brief, EGP was calculated by subtracting the exogenous glucose infusion rate (GIR) from the rate of disappearance of glucose (Rd) during the euglycemic hyperinsulinemic clamp:

$$EGP = Rd + Vglucose \times \Delta glucose/\Delta T - GIR$$

GIR is corrected by a space correction (DeFronzo et al. 1979) where Vglucose is the estimated glucose distribution volume (0.19 l/kg), Δglucose is the change in glucose from [^{18}F]FDG injection to the end of sampling (mmol/l), and ΔT is the time between [^{18}F]FDG injection and the end of sampling (min).

Glucose disappearance rate (Rd) was calculated using [^{18}F]FDG clearance corrected by tracer lost to urine (Iozzo et al. 2006) according to the following formula:

$$Rd = ((dose[^{18}F]FDG - urine[^{18}F]FDG)/AUC_{[18F]FDG}) * avg_{glucose}$$

Where dose [^{18}F]FDG is the activity of the injected [^{18}F]FDG, urine [^{18}F]FDG is [^{18}F]FDG secreted to urine from the tracer injection until voiding bladder at the end of the study, $AUC_{[18F]FDG}$ is the area under the curve representing [^{18}F]FDG from the tracer injection to infinity, and $avg_{glucose}$ is the average glycemia during the interval between the time of [^{18}F]FDG injection and the end of sampling.

4.7 Beta cell function (II)

ß-cell function was assessed from OGTT modeling. This model describes the relationship between insulin secretion rate (ISR, expressed in $pmol \cdot min^{-1} \cdot m^{-2}$) and glucose concentration as the sum of two components (Mari et al., 2002a; Mari et al., 2002b). The first component represents the dependence of ISR on glucose concentration through a dose-response function relating the two variables. From the dose-response, ß-cell glucose sensitivity (the slope) is calculated. The dose-response is modulated by a potentiation factor, accounting for various mechanisms (antecedent hyperglycemia, non-glucose substrates, gastro-intestinal hormones, neural modulation). The potentiation factor averages 1 during the test and expresses relative potentiation or inhibition of ISR; its excursion is quantified by the ratio between the two-hour and the baseline value (potentiation). The second ISR component represents the dependence of ISR on the rate of change of glucose concentration and is determined by a single parameter (rate sensitivity), which is related to early insulin release (Mari and Ferrannini 2008). The model parameters were estimated from glucose and C-peptide concentrations (using C-peptide deconvolution) (Van Cauter et al., 1992) as previously described (Mari et al., 2002b).

4.8 Insulin clearance

Insulin clearance was calculated from the OGTT as mean insulin secretion divided by mean insulin concentration (Camastra et al., 2005).

4.9 Blood measurements

Plasma glucose was measured in the laboratory of the Turku PET Centre in duplicate using the glucose oxidase technique (Analox GM7 or GM9, Analox Instruments Ltd., London, UK). Glycosylated hemoglobin (HbA1c) was measured with ion-exchange high performance liquid chromatography (Variant II Haemoglobin A1c, Bio-Rad Laboratories, CA, USA). Plasma insulin was determined by time-resolved immunofluorometric assay (AutoDELFIA, Perkin Elmer Life and Analytical Sciences). C-peptide was measured with electrochemiluminescence analyzer immunoassay (ECLIA) (Roche Diagnostics GmbH, Mannheim, Germany). Serum

FFA were measured with a photometric enzymatic assay (FFA-HR(2). Wako Chemicals GmbH, Neuss, Germany) on Modular P800 automatic analyzer (Roche Diagnostics, Mannheim, Germany). Serum high-sensitivity C-reactive protein (hs-CRP) was analyzed with the sandwich immunoassay method using an Innotrac Aio1 immunoanalyzer (Innotrac Diagnostics, Turku Finland). Serum adipokines were analyzed in duplicate by using Milliplex Human Serum Adipokine (Panel A) kit [cat.no HADK1-61K-A] containing interleukin-6 (IL-6), interleukin-8 (IL-8), tumor necrosis factor alpha (TNFα), and leptin.

4.10 Metabolomic measurements (I)

Metabolic biomarkers were quantified from the serum using high-throughput proton NMR metabolomics (Nightingale Health Ltd, Helsinki, Finland; University of Eastern Finland, Kuopio, Finland). This method provides simultaneous quantification of routine lipids, fatty acid composition, and various low-molecular metabolites including amino acids and, ketone bodies as well as lipoprotein subclass profiling with lipid concentrations within 14 subclasses. The 14 lipoprotein subclass sizes were defined as follows: extremely large VLDL with particle diameters from 75 nm upwards, five VLDL subclasses (average particle diameters of 64.0 nm, 53.6 nm, 44.5nm, 36.8 nm, and 31.3 nm), IDL (28.6 nm), three LDL subclasses (25.5 nm, 23.0 nm, and 18.7 nm), and four HDL subclasses (14.3 nm, 12.1 nm, 10.9 nm, and 8.7 nm). The following components of the lipoprotein subclasses were quantified: phospholipids, triglycerides, cholesterol, free cholesterol, and cholesterol esters. The mean sizes of VLDL, LDL, and HDL particles were calculated by weighting the corresponding subclass diameters with their particle concentrations. Details of the experimentation and applications of the NMR metabolomics platform have been discussed previously (Inouye et al. 2010; Soininen et al. 2015).

4.11 FLAIR MRI sequence to assess brain inflammation and variability of the method (III)

To measure mediobasal hypothalamic (MBH) gliosis, the signal intensity (SI) was retrospectively measured from coronally oriented fluid-attenuated inversion recovery (FLAIR) images from magnetic resonance imaging (MRI), as previously described (Kreutzer et al., 2017; Schur et al., 2015; Thaler et al., 2012). FLAIR images were gathered as part of the study protocol on a Philips 1.5T MRI scanner (Philips Ingenuity), with the following image parameters: repetition time: 11000 ms, echo time: 140 ms, inversion time: 2800 ms, slice thickness 5 mm. Briefly, circular regions of interest (ROIs, about 4 mm^2) were placed on one coronal slice onto MBH, which was identified as a bilateral most caudal brain region situated between the

optic chiasm anteriorly and the mamillary bodies posteriorly. The amygdala, visible on the same slice in the medial temporal lobe, was chosen as the reference region (ROI about 20 mm^2) for the normalization of MBH SI, and the MBH-amygdala SI ratio served as the primary outcome measure of hypothalamic gliosis. To examine whether SI findings were specific to MBH, the putamen was used as an internal control region (ROI about 20 mm^2), and putamen-amygdala ratios were calculated. All measurements were carried out by a board-certified staff neuroradiologist (J.H.). Thirty cases were also independently analyzed by a second neuroradiologist (M.N.), and between-rater reliability was assessed by determining the variability (absolute difference between measurements by two raters, divided by the average of those measurements), and by determining the intraclass correlation coefficients (ICC), where <0.5 is poor, 0.5-0.75 is moderate, 0.75-0.9 is good, and >0.9 is excellent reliability. We found low inter-rater variability (3.6%), suggesting low measurement error, and an ICC estimate of 0.63, suggesting moderate agreement.

4.12 Indirect calorimetry (III)

Energy expenditure was measured using indirect calorimetry (Deltatrac II; Datex-Ohmeda). Whole-body energy expenditure, substrate utilization rates, and respiratory quotients were calculated as previously described (Weir 1949).

4.13 Surgical procedure (I and III)

All surgeries were performed by the same team at Turku University Hospital. In brief, for RYGB a small gastric pouch of approximately 20-40 ml was created by dividing the upper part of the stomach. The jejunum was anastomosed to the gastric pouch approximately 50-70 cm distal to the ligament of Treitz. The alimentary limb was measured at 150 cm and a side-to-side jejunojejunal anastomosis was created between the alimentary and biliopancreatic limbs. Afterwards, the jejunum was transected between the two anastomoses. For LSG, the great curvature and the fundus were resected, leaving a tubular shaped stomach.

4.14 Statistical analysis

Data are presented as mean ± SD (or median [interquartile range IQR] for non-normally distributed variables). Statistical analysis at the voxel and cluster level was performed with statistical parametric mapping (SPM) (SPM12 toolbox for Matlab). Linear regressions were performed in SPM to evaluate correlations between BGU (and BFAU) and single regressors (EGP, insulin secretion rate, potentiation, ecc.) while controlling for confounding factors (in the SPM contrast, the controlling

variables were set to a value of 0). Between groups comparisons (obese vs. lean and obese before and after surgery) were performed in SPM with two-sample t-test and paired t-test, respectively. Brain glucose (and fatty acid) uptake values were extracted from the global ROI with Marsbar plug-in for Matlab and visualized with the single regressors using scatter-plot correlation coefficients (*r*). The statistical threshold in the SPM analysis was set at a cluster level and corrected with false discovery rate (FDR) with $p < 0.05$. Further statistical analyses were done using JMP version 13.0 (SAS Institute, Cary, NC, USA). A p value < 0.05 was considered statistically significant.

Associations between BGU and circulating metabolites were tested using Spearman correlations (Study I). Statistical analysis was performed using an R computing environment (version 3.4) (R Core Team 2017). Heatmaps were created with the gplots package (Warnes et al. 2016).

4.15 Ethics

A written informed consent was obtained from all study subjects prior to inclusion in the studies. All studies were approved by the ethical review committee of the Hospital District of Southwest Finland and carried out according to the principles of the Declaration of Helsinki, GMP, and GCP guidelines.

5 Results

5.1 Brain glucose uptake correlates positively with liver glucose production (I)

As expected, obese subjects had higher plasma glucose concentration, lipid profiles, and inflammatory markers at baseline compared to the age-matched lean controls. The anthropometric and biochemical characteristics of the two groups are listed in Table 2.

Table 2. Anthropometric and biochemical characteristics of the study participants.

	Controls	Obese		*p* value
		Pre	Post	
M/W	4/8	1/19	0/16	-
NGT/IGT/T2D	9/3/0	4/10/6	13/2/1*	<0.0001
Age (years)	43 ± 11	46 ± 9	47 ± 9	0.4
BMI ($kg \cdot m^{-2}$)	23.2 [3.0]	43.1 [2.5]	32.2 [3.1]*#	<0.0001
FM (%)	32.4 [9.1]	48.1 [1.7]	41.9 [3.0]*#	<0.0001
Fasting plasma glucose ($mmol \cdot L^{-1}$)	5.5 ± 0.4	6.2 ± 0.8	5.4 ± 0.5*	0.01
Insulin Clearance ($L \cdot min^{-1} \cdot m^{-2}$)	1.5 ± 0.3	1.1 ± 0.3	1.3 ± 0.3*	0.004
HbA_{1c} (%)	5.6 ± 0.3	5.8 ± 0.5	5.5 ± 0.3*	0.08
Leptin ($ng \cdot mL^{-1}$)	15.5 [14]	55.7 [23]	26.9 [15]*#	0.0002
IL-6 ($pg \cdot mL^{-1}$)	1.1 [1.2]	2.6 [2.0]	1.9 [0.6]*	0.02
CRP ($mg \cdot L^{-1}$)	0.8 [1.3]	3.2 [5.1]	1.0 [1.8]*	0.003
Total Cholesterol ($mmol \cdot L^{-1}$)	5.1 ± 0.8	4.4 ± 0.8	4.2 ± 0.5#	0.04
HDL Cholesterol ($mmol \cdot L^{-1}$)	1.9 ± 0.5	1.3 ± 0.2	1.5 ± 0.2*	0.003
LDL Cholesterol ($mmol \cdot L^{-1}$)	3.0 ± 0.7	2.8 ± 0.7	2.5 ± 0.5	0.5
Triglycerides ($mmol \cdot L^{-1}$)	0.9 ± 0.4	1.3 ± 0.4	0.9 ± 0.2*	0.006
ALT ($U \cdot L^{-1}$)	17 ± 7	31 ± 12	19 ± 10*	0.0007
gGT ($U \cdot L^{-1}$)	15 [13]	30 [18]	13 [8]	0.0006
Steady-state insulin ($pmol \cdot L^{-1}$)	392 ± 94	518 ± 190	467 ± 76#	0.04
Steady-state glucose ($mmol \cdot L^{-1}$)	5.1 [0.2]	5.0 [0.1]	5.2 [0.1]	0.4
M-value ($\mu mol \cdot kg_{FFM}^{-1} \cdot min^{-1}$)	67.3 [43.3]	25.2 [23.0]	52.1 [34.0]*#	<0.0001
Fasting EGP ($\mu mol \cdot kg_{FFM}^{-1} \cdot min^{-1}$)	15.49 [2.78]	14.82 [4.68]	14.76 [3.25]	0.8
Fasting EGP ($\mu mol \cdot min^{-1}$)	724 [142]	899 [311]	754 [236]*	0.0004
EGP clamp ($\mu mol \cdot kg_{FFM}^{-1} \cdot min^{-1}$)	0.27 [7.74]	6.20 [8.18]	3.6 [5.56]	0.03
EGP clamp ($\mu mol \cdot min^{-1}$)	12 [351]	390 [522]	208 [318]	0.006

entries are mean ± SD or median [interquartile range]; *p* value for the comparison obese pre *vs.* lean controls; * = *p* value < 0.05 for the comparison obese pre *vs.* obese post; #= *p* value < 0.05 for the comparison obese post *vs.* lean controls.

In the post absorptive state, BGU was not different between obese and lean subjects, and EGP was higher in the obese than the lean subjects. During the clamp, plasma glucose levels were well-matched between the two groups. Even though the exogenous insulin infusion was adjusted for body surface area, steady-state serum insulin levels were higher in the obese due to lower insulin clearance in this group. As expected, obese subjects also had lower M-value and higher insulin-suppressed EGP; the two parameters were reciprocally related (**Figure 10**).

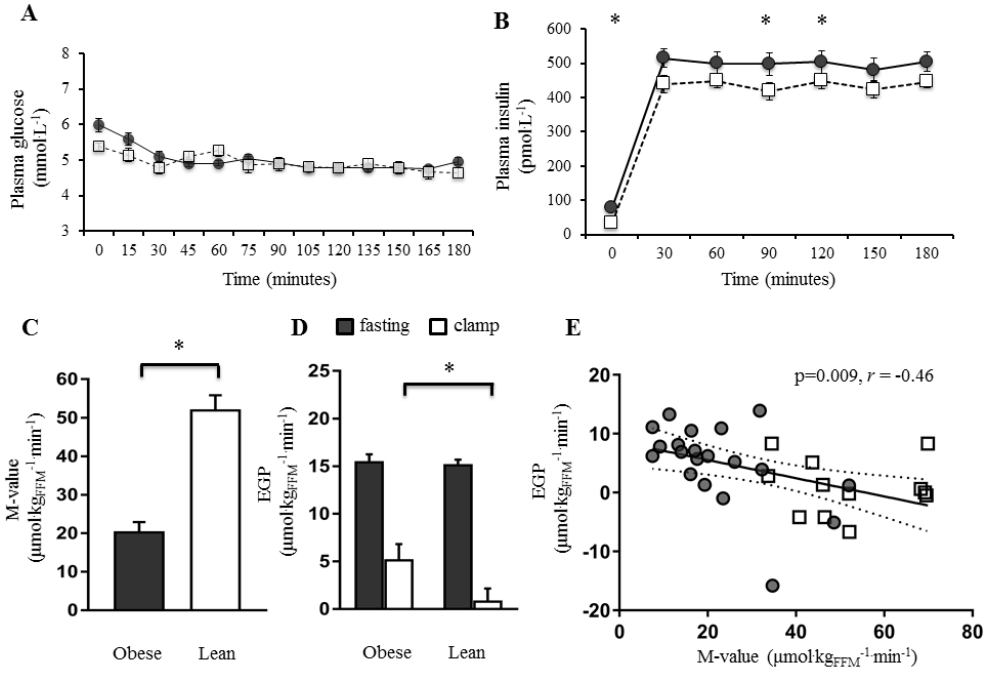

Figure 10. Plasma glucose levels were well-matched between the two study groups (A), but insulin levels were higher at some time-points in the obese group (indicated with *) (B). Compared to lean subjects, the obese subjects had lower M-value (C) and higher EGP (D), with the two measurements being reciprocally related (E).

Cross-sectionally, BGU during the clamp was higher in the obese compared to controls and correlated positively with insulin-suppressed EGP (r=0.51, p=0.003) (**Figure 11**). This association was driven by the obese group (r=0.60, p=0.006 in obese subjects, r=-0.1, p=0.7 in lean subjects). This association remained significant after accounting for BMI (r=0.66, p=0.009) or steady-state insulin (r=0.54, p=0.003). On the contrary, in the fasting state, BGU and EGP did not correlate.

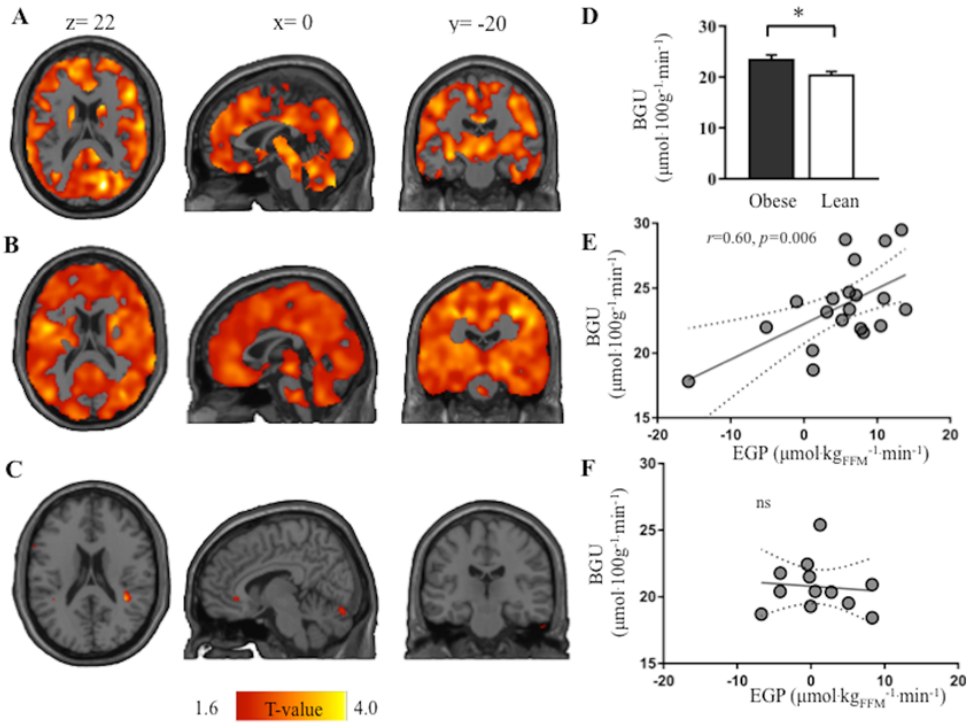

Figure 11. A: SPM two-sample t-test between obese subjects pre-operatively and controls. Marked brain areas show regions with significantly higher BGU in the obese subjects than controls. Higher t-values denote larger differences between the groups. P values < 0.05 cluster level, FDR corrected. D: corresponding boxplots showing the differences in BGU between the two groups. Data are mean ± SEM; * = p<0.05. B: SPM images of the association between BGU during clamp and insulin-suppressed EGP in the obese subjects pre-operatively. P values < 0.05 cluster level, FDR corrected. C: No association between BGU during clamp and EGP in lean controls. For images B and C marked brain areas show where the association between BGU and EGP was statistically significant. Higher t-values denote stronger association between BGU and EGP (color bar at the bottom). E, F: Corresponding scatterplots of the association between BGU and EGP in the obese and lean, respectively.

In 26 subjects (19 obese and 7 lean) who had IL-6 and CRP measurements taken, the measurements were positively associated with BGU (r=0.52, p=0.006 at the cluster level for IL-6 and r=0.52, p=0.007 at the whole-brain level for hs-CRP). Also, BGU during clamp was positively associated with the aromatic amino acid, phenylalanine (r=0.60, p=0.001) and the branched-chained amino acid leucine (r=0.59, p=0.002) (N=26) (**Figure 12**). The correlation between BGU and phenylalanine and leucine remained significant after adjusting for the M-value (r=0.68, p=0.01, and r=0.67, p=0.01, respectively).

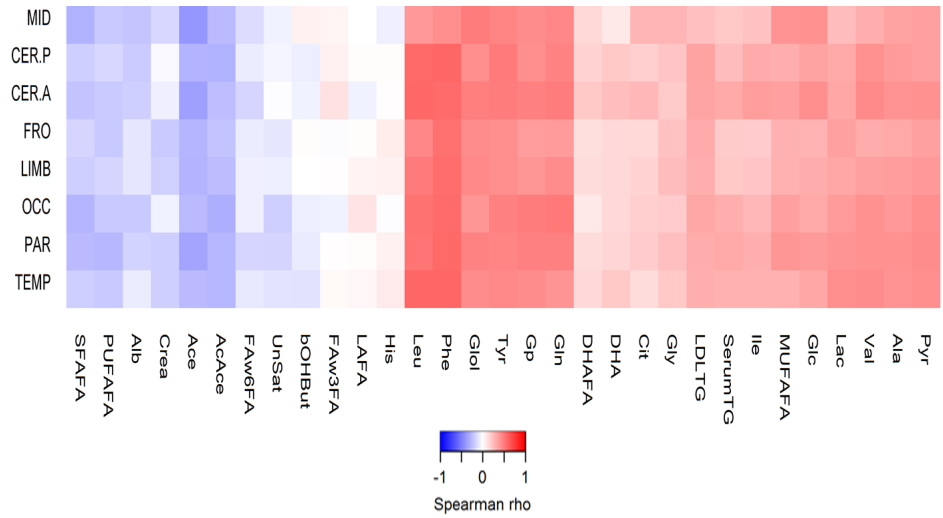

Figure 12. A: Spearman correlations between insulin-stimulated ROIs of BGU and fasting metabolites (N=26). CER-A, anterior cerebellum; CER-P, posterior cerebellum; FRO, frontal lobe; LIMB, limbic lobe; MID, midbrain; OCC, occipital lobe; PAR, parietal lobe; TEMP, temporal lobe. DHA, 22:6, docosahexaenoic acid; DHAFA, ratio of 22:6, docosahexaenoic acid to total fatty acids; FAw3, Omega-3 fatty acids; FAw3FA, ratio of Omega-3 fatty acids to total fatty acids; Glc, glucose; Gln, glutamine; Glol, glycerol; Gp, glycoprotein acetylation; HDLC, total cholesterol in HDL; HDL2C, total cholesterol in HDL2; His, histidine; LDLTG, triglycerides in LDL; Leu, leucine; MUFA, monounsaturated fatty acids; MUFAFA, ratio of monounsaturated fatty acids to total fatty acids; Phe, phenylalanine; PUFAFA, ratio of polyunsaturated fatty acids to total fatty acids; Pyr, pyruvate; Serum-TG, serum total triglycerides; SFAFA, ratio of saturated fatty acids to total fatty acids; Tyr, tyrosine; UnSat, estimated degree of unsaturation; VLDLC, total cholesterol in VLDL.

After surgery

Six months after surgery, obese subjects had achieved significant weight loss (~24% of their initial body weight), but their BMI remained significantly higher compared to the controls. The M-value doubled, and serum IL-6 and CRP levels decreased significantly. Fasting EGP decreased significantly, but insulin-suppressed EGP showed a small, non-significant decrease. BGU was decreased (~5%) but was still higher than in controls and positively associated with EGP (r=0.56, p=0.02) (**Figure 13**).

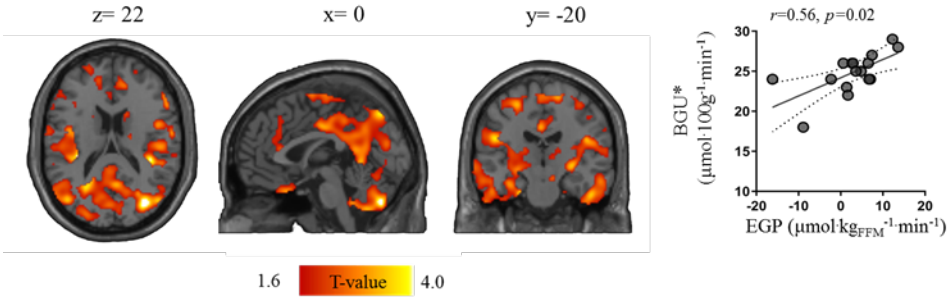

Figure 13. SPM images of the association between insulin-stimulated BGU and insulin-suppressed EGP in the obese subjects postoperatively and the corresponding scatterplot. In the scatterplot the mean BGU from the significant voxels only is presented (BGU*).

Follow-up

Patients were weight-stable at two and three years of follow-up (BMI: 32.1 [4.1] and 32.1 [3.8] kg/m2, respectively). A higher BGU during clamp before surgery was associated with a smaller improvement of fasting plasma glucose levels at two years (r=-0.63, p=0.006) (**Figure 14**). This association persisted after correcting for baseline BMI (r=-0.66, p=0.01) or M-value (r=-0.72, p=0.02) (N=17). In 13 subjects who had complete follow-up data for up to 3 years, higher baseline values of BGU during clamp were still predictive of smaller postoperative decrements of fasting glucose levels (r=-0.71, p=0.006). On the contrary, baseline BGU was unrelated to BMI or HbA_{1c} at follow-up.

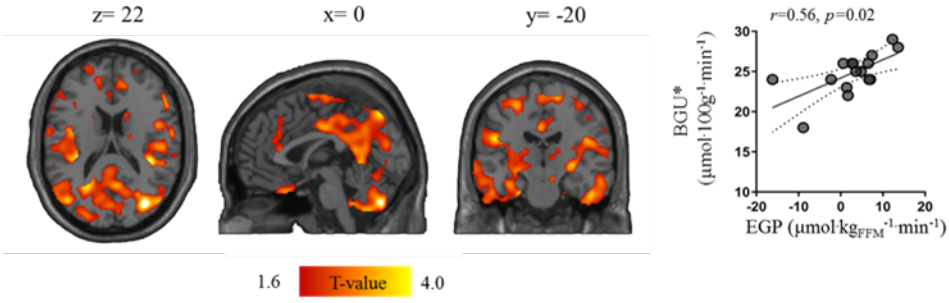

Figure 14. SPM images of the association between BGU during clamp at baseline and change in plasma glucose at two years of follow-up in 17 obese subjects and the corresponding scatterplot. P values <0.05 cluster level, FDR corrected

5.2 Brain glucose uptake correlates positively with parameters of beta cell function (II)

The characteristics of the study participants are reported in **Table 3**.

Table 3. Anthropometric and biochemical characteristics of the study participants.

	Clamp [^{18}F]FDG (a)		Fasting [^{18}F]FTHA (b)		Fasting [^{18}F]FDG (c)	
	Non-T2D	T2D	Non-T2D	T2D	Non-T2D	T2D
M/F	9/43	4/11	0/26	0/8	10/29	0/6
Age (years)	45 ± 10	49 ± 7	44 ± 12	45 ± 8	44 ± 9	54 ± 5*
BMI ($kg \cdot m^{-2}$)	27.4 [17.7]	34.0 [12.1]*	27.7 [17.8]	39.1 [18.0]*	32.0 [10.0]	41.5 [15.0]
HbA_{1c} (%)	5.5 [0.5]	5.9 [0.7]*	5.6 [0.6]	6.2 [1.0]*	5.8 [0.4]	6.8 [0.6]*
M value ($\mu mol \cdot kgFFM^{-1} \cdot min^{-1}$)	39.4 [30.0]	19.3 [14.7]*	-	-	32.6 [32.6]	19.8 [23.3]
Plasma insulin ($pmol \cdot L^{-1}$)	476 [221]	609 [161]	40 [47]	119 [13]*	53 [44]	112 [63]*
Serum FFA ($mmol.L^{-1}$)	0.05 [0.05]	0.1 [0.06]*	0.61 [0.40]	0.79 [0.44]	0.49 [0.31]	0.61 [0.26]
Basal ISR ($pmol \cdot min^{-1} \cdot m^{-2}$)	86 [55]	135 [38]*	81 [44]	152 [85]*	91 [66]	118 [72]
Total insulin output ($nmol \cdot m^{-2}$)	40 [22]	48 [16]	44 [18]	44 [11]	-	-
β-GS ($pmol \cdot min^{-1} \cdot m^{-2} \cdot mM^{-1}$)	119 [107]	48 [38]*	117 [101]	42 [40]*	-	-
Rate sensitivity ($pmol \cdot m^{-2} \cdot mM^{-1}$)	506 [1363]	651 [1057]	922 [1091]	349 [410]*	-	-
Potentiation ratio	1.3 [0.7]	1.3 [1.1]	1.4 [1.6]	1.2 [0.8]	-	-
Brain substrate uptake ($\mu mol \cdot 100g^{-1} \cdot min^{-1}$)#	25.7 [10.9]	28.3 [8.0]*	1.0 [0.6]	1.1 [0.8]	20.5 [5.4]	17.5 [4.1]

Entries are mean±SD, or median [IQR]; #glucose, or FFA as appropriate. * *p* value <0.05, for the comparison between non-T2D and T2D. BMI = body mass index; ISR = insulin secretion rate; β-GS = ß-cell glucose sensitivity; T2D = type 2 diabetes

Insulin-stimulated brain glucose uptake and whole body glucose disposal (dataset a)

Cross-sectionally (N=67), insulin-stimulated BGU correlated negatively with the degree of insulin sensitivity (M-value) (r=-0.40, p=0.001) and positively with the average (steady-state) FFA concentration (r=0.42, p=0.0007).

Brain glucose uptake and ß-cell function (dataset a and c)

Insulin-stimulated BGU correlated positively with basal ISR (r=0.44, p=0.0002) and total insulin output (r=0.36, p=0.003). Contrastingly, no significant association was

found between fasting brain glucose uptake and basal ISR (N=45). With regard to the dynamic parameters of ß-cell function, only potentiation (not ß-cell glucose sensitivity or rate sensitivity) was directly related to BGU (r=0.24, p=0.048).

These results were driven by the subjects not affected by T2D (non-T2D) because when we divided the population into non-T2D (N=52) and T2D (N=15), said associations remained significant only in the non-T2D (r=0.51, p=0.0008 for basal ISR and r=0.51, p=0.0008 for total insulin output) (**Figure 15)**.

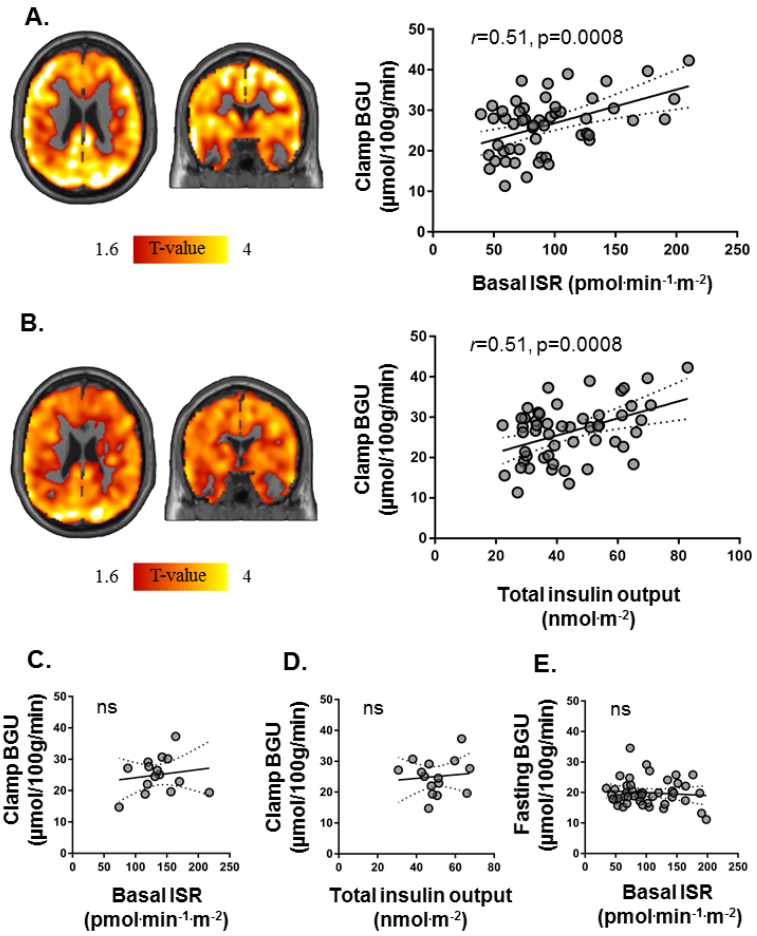

Figure 15. Brain clusters (as defined by FDR-corrected SPM two-sample t-test) for the association between brain glucose uptake (BGU) during clamp and basal insulin secretion rate (ISR) (A) and total insulin output (B) in non-T2D. No correlation between BGU during clamp and basal insulin secretion rate (ISR) (C) or total insulin output in T2D (D). No correlation between fasting BGU and basal insulin secretion rate (E). For the corresponding scatterplots, the global ROI was extracted and used.

Interestingly, potentiation behaved differently, and whereas BGU and potentiation were directly related in the 52 non-T2D (r=0.33, p=0.02), in the T2D group there was a significant inverse correlation between BGU and PFR (r=-0.61, p=0.02) (**Figure 16**).

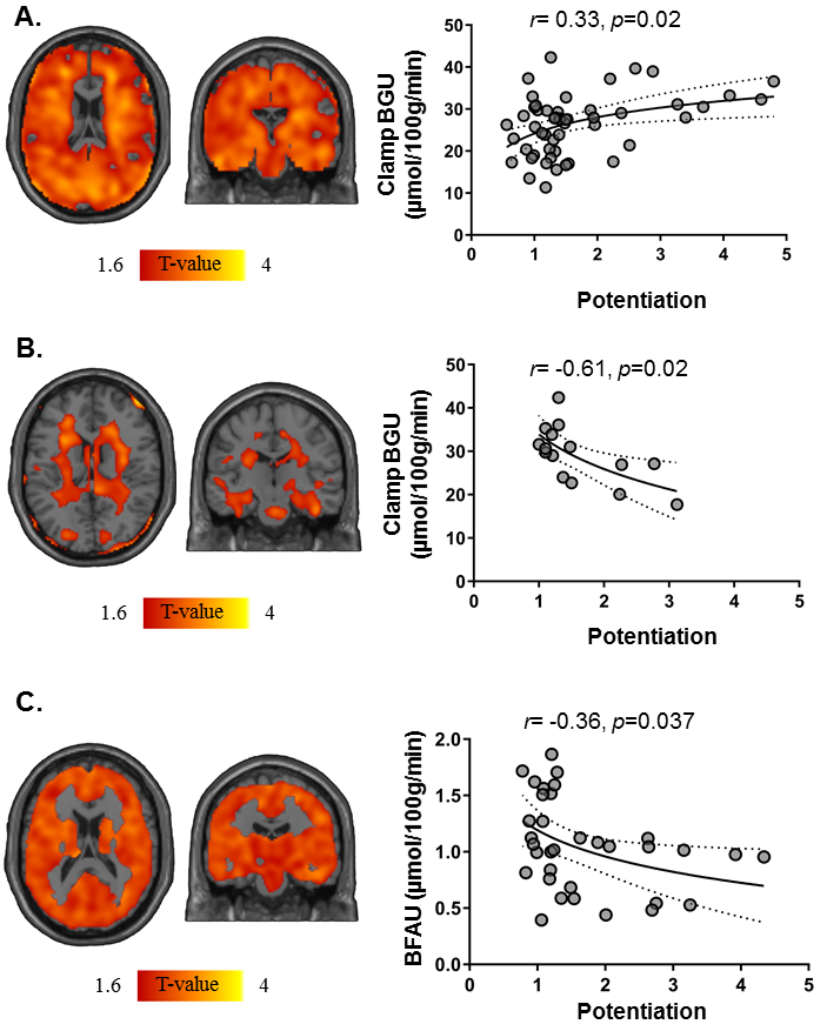

Figure 16. Brain clusters (as defined by FDR-corrected SPM one-sample t-test) for the association between brain glucose uptake (BGU) during clamp and potentiation of insulin secretion in non-T2D (A) and T2D (B) and the corresponding scatterplots. Brain clusters (as defined by FDR-corrected SPM one-sample t-test) for the association between brain fatty acid uptake (BFAU) and potentiation (C). Due to the non-global effects, the occipital ROI was extracted and used in the scatterplot

In the non-T2D group, we applied a stepwise selection approach in order to find the optimal models of prediction of BGU during clamp. In the models, we included possible confounders, such as the time interval from FDG injection to the brain scan, the fact that three different scanners were used, BMI, M-value, steady-state plasma insulin levels and one parameter of ß-cell function in use at the time. In all cases, the parameters of ß-cell function (basal ISR, total insulin output, and potentiation) were included in the optimal prediction models of BGU during clamp. In the same line, after partialing for insulin sensitivity (basal ISR, PFR) or BMI (for total insulin output), the associations between BGU and basal ISR (r=0.32, p= 0.024), PFR (r=0.44, p= 0.001) and total insulin output (r=0.37, p= 0.008) remained significant.

Regional findings

In the 52 non-T2D, the positive correlations between BGU and basal ISR as well as total insulin output were confirmed also in the various regions of interest examined (**Table 4**). The positive and negative correlations between BGU and PFR in non-T2D and in patients with T2D were also confirmed in most ROIs.

Table 4. Correlations between BGU and basal ISR, total insulin output, and potentiation *(dataset a)*.

	Basal ISR		**TIS**		**PFR**			
					non-T2D		**T2D**	
	p value	*r*	*p* value	*r*	*p* value	*rho*	*p* value	*rho*
Cerebellum Ant.	0.005	0.39	0.007	0.37	0.02	0.32	0.02	-0.61
Cerebellum Post.	0.007	0.37	0.007	0.37	0.02	0.33	0.04	-0.53
Occipital Lobe	0.002	0.43	0.002	0.43	0.01	0.34	0.02	-0.60
Parietal Lobe	0.001	0.45	0.001	0.46	0.03	0.31	ns	-
Temporal Lobe	0.003	0.41	0.005	0.39	0.03	0.30	0.03	-0.56
Frontal Lobe	0.002	0.43	0.002	0.42	0.03	0.30	ns	-
Limbic Lobe	0.002	0.42	0.005	0.39	0.03	0.31	0.03	-0.56
Midbrain	0.002	0.43	0.004	0.40	0.04	0.29	0.02	-0.60

r: correlation coefficient; *rho:* Spearman correlation coefficient. Cerebellum Ant= Cerebellum anterior; Cerebellum Post=Cerebellum posterior

Brain FFA uptake and ß-cell function (b)

Brain FFA uptake (BFAU) was positively associated with BMI (r=0.5, p=0.003) and other measures of adiposity. BFAU also correlated with basal ISR (r=0.39, p=0.02) and, in an inverse manner, with potentiation (r=-0.36, p=0.04) (**Figure 16C**). Similar trends of these associations were found also when dividing the population into non-

T2D and subjects with T2D (N=8), even though the associations in the T2D group did not reach statistical significance probably because of low numerosity.

Regional findings

The correlations between BFAU and the aforementioned parameters of ß-cell function were confirmed also in the various regions of interest examined (**Table 5**).

Table 5. Correlations between BFAU and BISR and Potentiation.

	Basal ISR		**Potentiation**	
	p-value	*r*	*p*-value	*rho*
Cerebellum Anterior	0.03	0.38	0.02	-0.41
Cerebellum Posterior	0.04	0.36	0.04	-0.35
Occipital Lobe	0.03	0.38	0.02	-0.41
Parietal Lobe	0.02	0.39	0.01	-0.42
Temporal Lobe	0.02	0.39	0.01	-0.43
Frontal Lobe	0.02	0.39	0.01	-0.42
Limbic Lobe	0.01	0.42	0.01	-0.42
Midbrain	0.03	0.38	0.02	-0.39

r: correlation coefficient; *rho:* Spearman correlation coefficient

The following scheme summarizes the found associations (**Figure 17**).

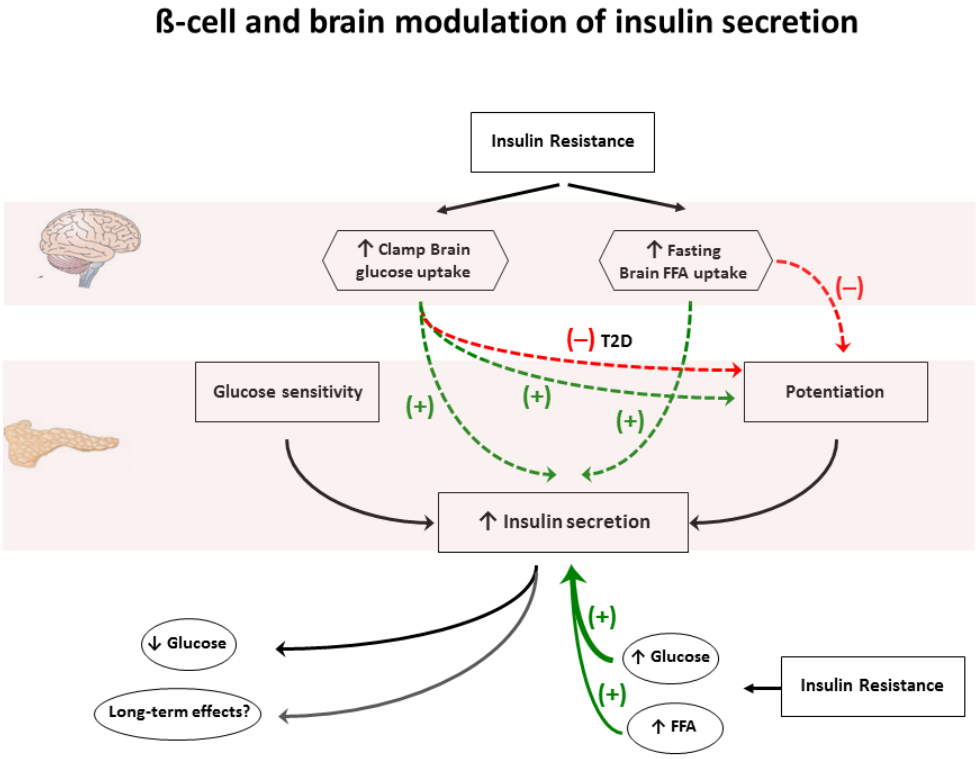

Figure 17. Schematic representation of the separate influence of substrate levels on insulin secretion; directly on the ß-cell and indirectly via brain substrate uptake. Assuming that the brain "drives" the observed correlations, increased BGU in conditions of insulin stimulation may lead to enhanced insulin secretion in non-T2D and increased or decreased potentiation in non-T2D and T2D, respectively. Increased BFAU during fasting may stimulate insulin secretion, but downregulate potentiation. The net effect of these phenomena would result in enhanced insulin secretion in non-T2D, which in the short term would restore normal plasma glucose levels. However, an activated brain-pancreas axis might also have long-term effects. In T2D, the brain's control over insulin secretion seems either lost or reversed (see also text).

5.3 Brain fatty acid uptake is higher in obese subjects, but it does not decrease six months after bariatric surgery (III).

Clinical and metabolic characteristics of the study participants

By definition, obese participants had higher measures of adiposity (WHR, fat mass, and BMI), higher fasting FFA and glycerol levels, and worse insulin sensitivity, compared to age-matched lean controls. Obese participants also had high circulating inflammatory markers (**Table 6**).

Table 6. Anthropometric and biochemical characteristics of the study subjects.

	Controls (n = 14)	Obese		
		Before (n = 24)	After (n = 21)	*p*°
Age (years)	45 ± 12	43 ± 10	-	-
BMI (kg/m^2)	22.6 ± 2.8	41.1 ± 4.2*	31.8 ± 4.2#	<0.0001
WHR (cm/cm)	0.77 ± 0.05	0.89 ± 0.07*	0.87 ± 0.09#	0.04
Fat mass (kg)	19 ± 6	56 ± 10*	37 ± 9#	<0.0001
Fat-free mass (kg)	42 ± 4	56 ± 9*	49 ± 6#	<0.0001
Triglycerides (mmol·L^{-1})	0.66 ± 0.32	1.18 ± 0.42*	1.09 ± 0.54#	ns
Glucose (mmol·L^{-1})	5.13 ± 0.34	5.71 ± 1.03*	5.30 ± 0.79	ns
Insulin (μU·mL^{-1})	3.0 [3.5]	9.5 [10.8]*	4.0 [3.0]	(0.06)
OGIS (ml·min^{-1}·m^{-2})	426 [91]	351 [67] *	444 [63]	<0.0001
HbA_{1c} (%)	5.6±0.3	6.0±0.7*	5.4±0.4	<0.0001
FFA (mmol·L^{-1})	0.55 ± 0.17	0.80 ± 0.22*	0.77 ± 0.17#	ns
Glycerol (μmol/L)	67 ± 23	113 ± 31*	108 ± 53#	0.01
hs-CRP (mg/L)	0.4 [0.6]	2.9 [3.8]*	0.9 [1.4]#	0.003
IL-8 (pg/ml)	4.14 [1.5]	4.6 [2.6]	4.4 [2.3]	ns
TNF-α (pg/ml)	2.4 [1.8]	4.4 [1.6]*	3.7 [1.9]	0.07
Leptin (ng/ml)	5.3 [5.3]	36.8 [21.3]*	15.4 [14.2]	<0.0001

Data are mean ± SD or median [IQR]; * $p < 0.05$ obese *vs.* controls; ° after *vs.* before surgery; # $p < 0.05$ obese after surgery *vs.* controls.

Before surgery

Brain FFA uptake was higher in the obese subjects than in the lean subjects (1.12 [0.61] *vs.* 0.72 [0.50] μmol·100g^{-1}·min^{-1}, p=0.002) (**Figure 18**). This increase was driven by higher FFA availability (0.80 ± 0.22 *vs.* 0.55 ± 0.17 mmol/L, p=0.001) as the fractional uptake rates were similar in the two groups (0.017 [0.005] *vs.* 0.018 [0.006] min^{-1} in the obese and in the lean subjects, respectively, ns). In contrast, the hypothalamus/amygdala FLAIR ratio did not differ between obese and control subjects (**Table 7**).

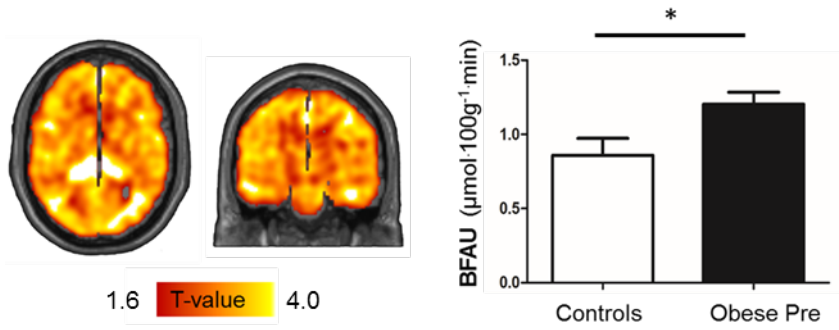

Figure 18. Brain clusters (as defined by FDR-corrected SPM one-sample *t*-test) for the comparison of brain fatty acid uptake (BFAU) between the two groups, and the corresponding bar graphs. The global ROI was extracted and used.

Table 7. Brain fatty acid uptake and the FLAIR hypothalamus/amygdala signal ratio.

	Controls (n=14)	Obese		*p**
		Before (n=24)	After (n=21)	
Global (µmol/100g/min)	0.72 [0.50]	1.12 [0.61]	1.09 [0.39]#	0.002
Cerebellum ant. (µmol/100g/min)	0.77 [0.57]	1.32 [0.75]	1.21 [0.49]#	0.001
Cerebellum post.(µmol/100g/min)	0.75 [0.61]	1.19 [0.73]	1.13 [0.48]	0.006
Frontal Lobe (µmol/100g/min)	0.67 [0.50]	1.04 [0.55]	0.99 [0.34]#	0.002
Limbic Lobe (µmol/100g/min)	0.71 [0.48]	1.11 [0.61]	1.06 [0.45]#	0.002
Midbrain (µmol/100g/min)	0.75 [0.52]	1.21 [0.71]	1.12 [0.42]#	0.002
Occipital Lobe (µmol/100g/min)	0.79 [0.55]	1.21 [0.65]	1.17 [0.40]#	0.003
Parietal Lobe (µmol/100g/min)	0.75 [0.53]	1.17 [0.64]	1.14 [0.39]#	0.001
Temporal Lobe (µmol/100g/min)	0.72 [0.48]	1.09 [0.58]	1.05 [0.38]#	0.002
Hypothalamus/amygdala signal	1.07 [0.04]	1.07 [0.08]	1.07 [0.09]	ns

Data are median [IQR]; *obese *vs.* controls; ° $p < 0.05$ after *vs.* before surgery; # $p < 0.05$ obese after surgery *vs.* controls

After surgery

Post-surgical data were available for 21 subjects since three subjects did not undergo surgery. Six months after the operation participants had lost a significant amount of body weight (26 ± 8 kg). Insulin sensitivity (as indexed by OGIS), HbA_{1c} levels, and circulating inflammatory markers had improved (**Table 6**). Because of the ongoing catabolic state, serum FFA levels were not decreased (0.80 ± 0.22 *vs.* 0.77 ± 0.17 mmol/L, ns). BFAU showed only a small, but not statistically significant, decrease (**Figure 19**). The hypothalamus/amygdala FLAIR ratio was unchanged.

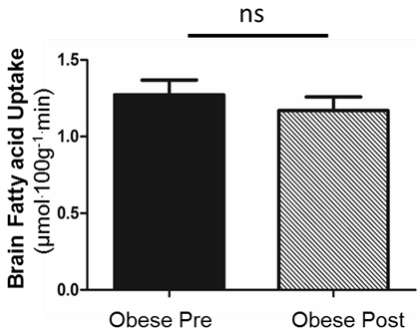

Figure 19. No difference in BFAU was found six months after bariatric surgery. The global ROI was extracted and used.

Correlations

Cross-sectionally, baseline BFAU was positively associated with BMI (r=0.47, p=0.003) and other markers of adiposity such as fat mass (r=0.45, p=0.006) and leptin (r=0.54, p=0.0008), and negatively associated with OGIS (r=-0.45, p=0.007). In contrast, the hypothalamus/amygdala FLAIR ratio did not correlate with BMI, circulating inflammatory markers, or BFAU (**Figure 20**).

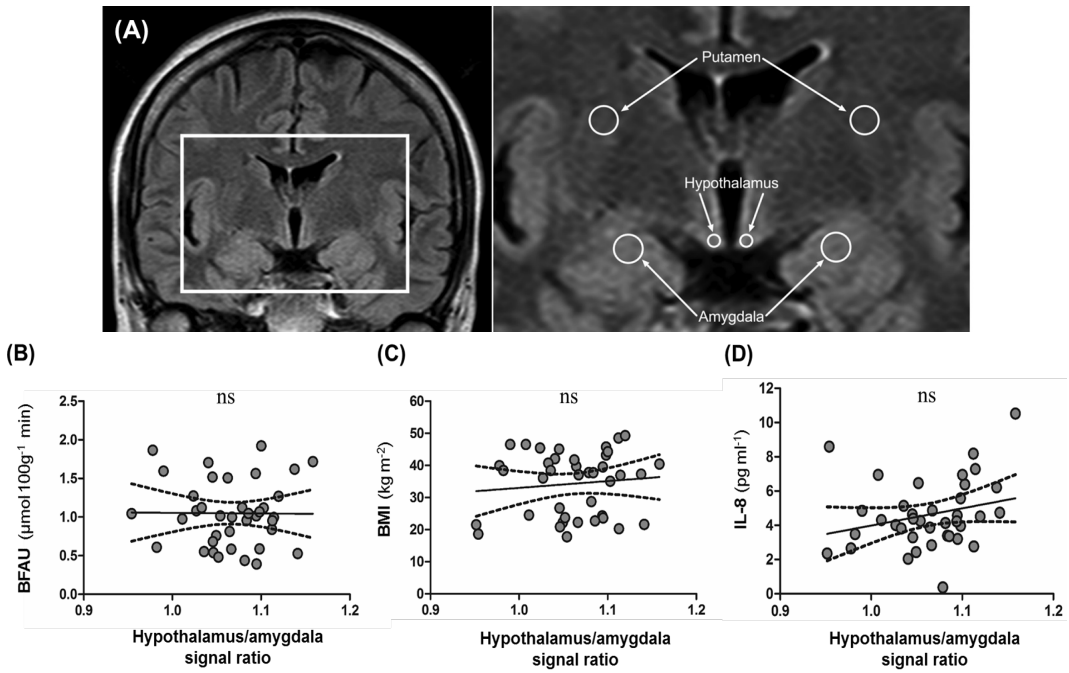

Figure 20. (**A**) A Flair images showing the region of interest positioning. The hypothalamus/ amygdala signal ratio did not correlate with BFAU, BMI, or IL-8 (**B-D**).

In the 18 subjects of whom we had follow-up data, baseline BFAU predicted higher plasma glucose levels at two years of follow up (**Figure 21**). The association remained significant after adjusting for baseline plasma glucose levels.

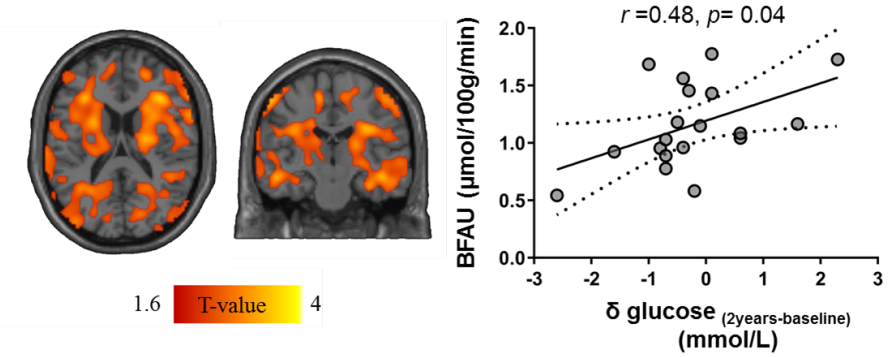

Figure 21. Brain clusters (as defined by FDR-corrected SPM one-sample *t*-test) for the association between (BFAU) and δ glucose at two years follow-up. The global ROI was extracted and used.

Since in the same PET study radioactivity from several organs/tissues was acquired, it is of interest to compare FFA uptake across different tissues. Per unit tissue mass, the brain was the 4th tissue in order of magnitude to use FFAs after the liver, heart, and kidney (**Figure 22**). However, by multiplying tissue uptake rates by the respective total mass, the contribution of the brain in total FFA uptake becomes marginal and similar in magnitude to visceral fat.

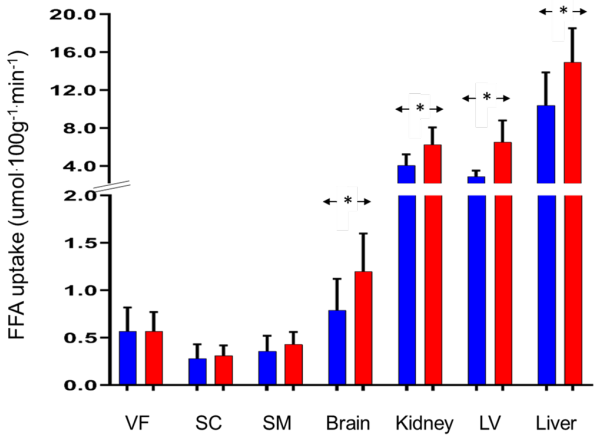

Figure 22. FFA uptake in several tissues measured in the same subjects. Brain FFA uptake per unit tissue mass is fourth after hepatic, cardiac and renal FFA uptake. Obese (red colour); lean controls (blue). * indicates p < 0.05 between obese and lean individuals. SC: abdominal subcutaneous fat, VF: visceral fat, SM: skeletal muscle, LV: left ventricle. Entries are mean±SE.

6 Discussion

There are several lines of research in a preclinical setting that have shown that the brain is involved in the control of whole-body homeostasis, and more specifically of the determinants of glucose tolerance. Human data are scanty, but necessary in order to translate these findings into humans, and gain further insight into the pathophysiology of metabolic diseases, which may eventually lead to the discovery of new potential treatments. The work in this thesis focused on studying the role of the brain in the orchestration of whole-body homeostasis. We used positron emission tomography and two tracers ([^{18}F]FDG and [^{18}F]FTHA) in order to study the connections of the brain to the peripheral determinants of glucose tolerance, namely insulin sensitivity and insulin secretion. Moreover in two different datasets we were able to see that high brain substrate utilization (glucose and fatty acids) predicts a worse glycemic control at follow-up.

Regarding the association between BGU and EGP (study I), we found that this brain-liver axis was present only in obese/insulin resistant subjects, but not in the lean controls. Similar findings were also reported from our group in another population of obese, middle-aged men (Latva-Rasku et al., 2017). The association between BGU and EGP persisted also after significant weight loss, six months after BS. Of note, even though the obese had achieved significant weight loss at the time of the post-operative studies, they still remained obese (mean BMI 33.1±3.8 kg·m^{-2}). This finding seems to be in line with results from experimental settings where intranasal insulin has been applied and EGP has been measured with the gold-standard of D-[6,6-2H]glucose infusion, whereby it was shown that on top of the euglycemic hyperinsulinemic clamp, intranasal insulin application suppresses EGP in lean but not in overweight subjects (Heni et al., 2017). Thus, if we combine the results of the two different groups, which used different neuroimaging approaches, it emerges that in lean (insulin sensitive subjects) there is no association between BGU and EGP, and when intranasal insulin is given, EGP is suppressed. On the contrary, in the obese (insulin resistant) subjects in which we found a positive association between BGU and EGP, intranasal insulin does not suppress EGP, indicating insulin resistance of the brain-liver axis. Assuming that the brain drives the observed association, one may hypothesize that the brain is driving the increased

EGP in the obese, and it is resistant to insulin to suppress EGP after intranasal insulin administration. It should also be noted that the Tubinghen group has also shown that during fasting conditions intranasal insulin application does not affect EGP (Gancheva et al., 2015), and also in our data BGU and EGP in the fasting state do not correlate.

Taken together, one might hypothesize that an important prerequisite for this brain-liver axis to be present are plasma insulin levels in the post-meal range. Of course, the exact mechanism for this crosstalk in humans is not known. Preclinical data suggest, though, that the phosphatidylinositol-3-kinase (PI3K) pathway is involved since in rats the effect of systemic high insulin levels on suppressing EGP was abolished after the ICV administration of PI3K inhibitors (Obici et al., 2002a). In that study, a similar effect on abolishing the EGP suppression was seen after central administration of antibodies against insulin or against the insulin receptor, but not when an antagonist of the mitogen-activated protein (MAP) kinase was given (Obici et al., 2002a). It has also been shown that activation of the hypothalamic K_{ATP} channels is involved in the suppression of EGP (Pocai et al., 2005). Other lines of research have provided evidence that central glucose sensing, involving glucose-regulated neurons as well as astrocytes, may also modulate EGP (Marty et al., 2007).

Of interest, baseline insulin-stimulated BGU predicted worse glycemic control at two and three years of follow-up (after also accounting for baseline plasma glucose levels). On the contrary insulin-stimulated BGU did not predict δBMI, δBW, or δHbA_{1c} at follow-up. Thus, insulin-stimulated BGU predicted only plasma glycemia, i.e. the parameter most dependent on EGP.

Similar findings of baseline brain substrate uptake predicting worse glycemic control at two years of follow-up were found also in the third study, where a similar group of morbidly obese women was studied before and after BS. The difference was that this time we had measured brain fatty acid uptake, during fasting conditions. These data suggest that high brain substrate uptake can predict, and perhaps lead to, metabolic deterioration in the future. Other research groups using different techniques have provided similar evidence. For instance, in the TULIP study, (an intervention study with lifestyle modification targeting weight loss), it was shown that central insulin resistance (defined in this study as blunted cerebrocortical insulin effect assessed by magnetoencephalography) was associated with a smaller decrease in total and visceral adipose tissue and fasting plasma glucose levels as well as worse adherence to the lifestyle recommendations (Tschritter et al., 2012). In an extended follow-up of nearly 10 years, the same group showed that central insulin resistance at baseline predicted weight regain (Kullmann et al., 2020).

Of course, as it will also be discussed in the limitations section, correlations do not prove cause-effect. On the other hand, it is of interest that both these two datasets showed this prediction of fasting glycemia. Studies with longer follow-up are

needed, to evaluate whether baseline high brain substrate uptake predicts worse metabolic outcome in the future. Similar longitudinal studies in subjects who have not undergone BS, are currently few and warranted.

Regarding the association between BGU and the parameters of ß-cell function (study II), there is mounting preclinical evidence (already 50-60 years old), suggesting that the brain may also influence insulin secretion. We also addressed whether brain substrate uptake associates with insulin secretion. For these studies in order to increase statistical power, we pooled and re-analyzed the data of all subjects in the same way from whom brain [^{18}F]FDG radioactivity was acquired, and who also underwent an OGTT with adequate blood sampling (at least 0, 30, 60, 90, 120) for OGTT modeling.

Based on the data of dataset (a), we found that insulin-stimulated BGU in non-T2D correlated positively with BISR, TIS, and potentiation. No associations were found regarding BGU and insulin secretion in a small group of 15 subjects with T2D. Regarding BISR and TIS, the correlations with insulin-stimulated BGU may be expected since in insulin resistance both increased insulin secretion and increased insulin-stimulated BGU have been reported. Of interest though, our results remained significant when accounting for the degree of insulin sensitivity. Furthermore, brain glucose uptake was also directly related to potentiation of insulin release in non-T2D (also after controlling for insulin resistance), and inversely in subjects with T2D. These correlations between brain substrate uptake and potentiation are of particular interest, since apart from the antecedent glycaemia and the incretins a neural factor has been also suggested to account for potentiation. Moreover, subjects with T2D, had an inverse correlation between BGU and PFR, thus the patterns of associations were clearly different for potentiation in subjects with T2D and non-T2D. Collectively, therefore, these results are compatible with the notion that ß-cell function may be modulated by the brain. In T2D this ‘’brain control’’ is either lost or reversed. This suggestion is in line with growing evidence that points to an alternative course in the natural history of glucose intolerance, whereby insulin hypersecretion may occur independently of insulin resistance (Trico et al., 2018) as a result of influences deriving from the central nervous system.

After detecting these findings when using [^{18}F]FDG-PET, we hypothesized that brain substrate uptake when using a fatty acid tracer could also correlate with the parameters of ß-cell function. We hypothesized so, because FFA are known to stimulate insulin secretion through direct effect on the pancreas (Rebelos et al., 2015). However, fatty acids also cross the BBB and have central effects. The current [^{18}F]FTHA-PET data show that brain FFA uptake under fasting conditions is directly associated with basal insulin secretion rate and negatively associated with potentiation. Thus, the uptake of glucose under insulinized conditions and the uptake of FFA under fasting conditions appear to be co-stimulatory signals in the brain for

insulin release. However, brain FFA uptake is a negative signal for potentiation of insulin release. This disassociation of substrate influence on insulin secretion vs. potentiation of insulin secretion is supported by recent data showing that potentiation of insulin release is impaired in insulin resistant individuals (who typically have elevated FFA levels) (Rebelos et al., 2017), and that acute elevations of plasma FFA impair incretin-induced potentiation of insulin release (Astiarraga et al., 2018). The idea of a separate influence of substrate levels on insulin secretion – directly on the ß-cell and indirectly via brain substrate uptake – is schematically summarized in **Figure 17**.

In dataset (c) of this study (study II), we assessed whether BGU during fasting correlates with BISR, but no such association was found. Thus, the associations between brain substrate uptake and the parameters of ß-cell function were found only in conditions where insulin resistance has an effect on up regulating brain substrate uptake (clamp conditions when studying BGU, fasting conditions when studying BFAU).

It is possible that the increased glucose availability to selected brain regions induced by insulin is read as a signal to upgrade global ß-cell function in order to defend/restore normal glucose homeostasis. In the fasting state, on the other hand, the increased brain FFA uptake restrains ß-cell function by downgrading potentiation. This interpretation (outlined in **Figure 17**) is based on associations and is, therefore, speculative. However, there is supportive evidence in the literature. Even though our data do not include any information with long follow-up, one might hypothesize that the brain-pancreas axis could have beneficial short-term effects restoring normal plasma glucose levels, but in the long term, it might ultimately contribute to the worsening of insulin resistance and/or ß-cell overload (**Figure 17**).

The mechanism of the brain- pancreas axis that we report is not known. Animal studies, though, have shown that astrocytes are involved in the control of both insulin and glucagon secretion after intracarotid injection of glucose and an intracerebroventricular injection of 2-deoxy-D-glucose, respectively (Guillod-Maximin et al., 2004; Marty et al., 2005).

In the last study (study III), we have shown that morbidly obese subjects have higher brain fatty acid uptake than lean individuals. Thus, we replicated and extended our original findings regarding metabolic syndrome (Karmi et al., 2010). In our previous study, the lean group consisted of men only, whereas the metabolic syndrome group consisted of both men and women. For this reason, we could not rule out differences in BFAU between genders. Because women undergo bariatric surgery more frequently than men, we investigated differences in morbidly obese vs. lean women only.

Brain FFA uptake ranged from 0.3-1.3 $\mu mol \cdot 100mL^{-1} \cdot min^{-1}$, which translates to a whole-brain uptake of 4-14 $\mu mol \cdot min^{-1}$. The fate of the uptaken FFAs from the

brain, is not completely known, but as discussed by Schönfeld and Reiser in their elegant review (Schonfeld and Reiser 2013), brain fatty acids can be either esterified to membrane lipids or undergo β-oxidation in the mitochondria. Furthermore, the authors argue that excessive oxidation of fatty acids could be detrimental to the "economy" of the brain cells. Accordingly, our previous study using both [^{18}F]-FTHA-PET and [^{11}C]-palmitate-PET (the first tracking total FFA uptake, the latter non-oxidative metabolism) concluded that not all of the uptaken fatty acids are oxidized by the brain (Karmi et al., 2010). In that study the oxidative part of FFA uptake (subtracting the non-oxidative metabolism from the total FFA uptake) would be roughly 70% of the total FFA uptake. On the other hand, if we take the average figure of 9 μmol·min^{-1} of brain FFA uptake from our data and we consider the $CMRO_2$ (~140 μmol/100g/min) and CBF (~44 mL/100g/min) values reported in the study by Goyal et al. (see also page 18) (Goyal et al., 2017) assuming a normal hematocrit of 0.45 and a brain volume of ~1400 ml, it emerges that if FFAs were completely oxidized by the brain, they would require ~202 μmol/min of O_2. However, the complete oxidation of 22 μmol/100g/min glucose, which is the average BGU under fasting conditions that Goyal et al. reported, leaves only 112 μmol/min of O_2 consumption unaccounted for (considering an oxygen to glucose ratio close to 6) and potentially attributable to other substances. Thus, based on these calculations, approximately half of the uptaken FFA from the brain is used for non-oxidative purposes. In both calculations, several assumptions, though, are made, which may explain why the estimated percentages of oxidative fatty acid uptake do not perfectly match. Moreover, since, in this PET study, fatty acid uptake rates were quantified during the same PET session from several tissues (including skeletal muscle, liver, heart and adipose tissue), we were able to compare the contribution of each tissue on the handling of FFA. Using the fatty acid analog [^{18}F]FTHA, we found that brain FFA uptake ranges between 0.3-1.3 μmol·100mL^{-1}·min^{-1}, which translates to a whole-brain uptake of 4-14 μmol·min^{-1}. By comparison with previous PET studies using [^{18}F]FTHA (Dadson et al., 2017; Hannukainen et al., 2018; Immonen et al., 2018; Rebelos et al., 2019), we can conclude that the brain has a relatively high tissue-specific FFA uptake (fourth after liver, kidney and heart but before adipose tissue or resting skeletal muscle). (**Figure 22**).

In all the studies presented in this thesis, we have hypothesized that the results could be mediated (at least to some extent) through astrocytes. This "astrocyte-centric" approach derives from the astrocytes' characteristic of representing the energy hubs of the brain. There are several reasons for taking this "astrocyte-centric" approach. First, astrocytes express several hormonal receptors, among which GLP-1, glucagon, and insulin, and have been shown in preclinical studies to participate in the handling of both insulin secretion, and EGP. Second, a recent publication has shown that the glucose uptake that is measured with [^{18}F]FDG-PET is driven by

astrocytes (Zimmer et al., 2017). This is in accord with what was originally proposed as the astrocyte-neuron lactate shuttle (ANLS), whereby astrocytes convert glucose into lactate and supply lactate to neurons (Pellerin and Magistretti 1994). As discussed in the introduction, this metabolic paradigm is controversial. However, the controversy mainly regards how the shuttle is closed, but that glucose is taken up by astrocytes and that they provide lactate to neurons seems a consolidated finding. Third, another well-known fact about astrocytes, is that in case of neuroinflammation, they proliferate and they become activated, a phenomenon known as astrogliosis. It is consolidated that obesity is linked with low-grade systemic inflammation (Hotamisligil 2006). However, animal studies have shown that a high-fat diet induces rapid neuroinflammation; in fact this process is so quick that it precedes the development of systemic inflammation (Thaler et al., 2012). Altogether, a plausible interpretation of our data could be that the increased brain glucose uptake in obesity is, at least in part, due to obesity-induced astrocyte proliferation.

In this respect, in Study III we analyzed the FLAIR MRI hypothalamus/ amygdala hyperintensity signal. This signal has been described to depict central inflammation. However, it is not specific, since similar MRI hyperintensities have been described also with edema, infection, and tumors which can have a similar appearance (Thaler et al., 2012). Moreover, it is not clear whether it is supposed to represent absolute hypothalamic inflammation or relative to amygdala hypothalamic inflammation. We hypothesized that BFAU could also be attributed to central inflammation, considering that the astrocytes are the main handler of fatty acids in the CNS. Contrary to our hypothesis, we did not find any association between BFAU and the hypothalamus/amygdala signal ratio. Moreover, we were not able to reproduce the previous findings by other groups regarding BMI and inflammatory markers (Schur et al., 2015; Thaler et al., 2012). This discrepancy could, in part be attributed to technical reasons. The hypothalamus is a very small brain region, and our FLAIR-MRI protocol was designed to cover the whole brain with 5-mm thick slices. These relatively thick slices may have caused ROI malpositioning and precluded sensitivity for subtle changes in the hypothalamic FLAIR signal. We found a small measurement error (inter-rater variability), yet only moderate intraclass correlations (0.63). Previous studies have not assessed the reliability of hypothalamic FLAIR measurements. This pattern of results suggests insufficient between-subject variability (i.e., identifiability of individuals) to make this ratio an optimal biomarker in metabolic studies. Apart from the pros and the limitations of this method, our hypothesis of neuroinflammation would require an imaging method that can assess the whole brain, and not be restricted to the hypothalamus. This is both because astrocytes are widely distributed in the CNS and also because the increased BGU in obese subjects is global and not restricted to the hypothalamic region.

6.1 Strengths, limitations

The strengths of the current studies are their relatively big numbers of study subjects, across a wide range of age, BMI, and insulin sensitivity. Baseline and follow-up data were combined showing that high brain substrate at baseline predicts metabolic outcome at follow-up, thus further underlying the importance of studying brain metabolic rates in humans. Moreover, the fact that state-of-the art techniques, such as positron emission tomography and the euglycemic hyperinsulinemic clamp have been applied in studying in vivo metabolism in humans, is a considerable strength.
One of the main limitations of the presented studies (I- II) is that they mainly presented correlational data and thus, cannot prove causality.

Still, while working on these data important deepening of our understanding has occurred. Based on the preliminary results from study I, and available literature, we formulated the hypothesis that the increased BGU in the obese/insulin resistant subjects could be driven by central inflammation. Based on this hypothesis, we are already conducting a clinical and preclinical study to address whether a) central inflammation occurs in morbidly obese subjects, b) whether the increased BGU is due to central inflammation, and c) whether central inflammation improves after significant weight loss.

In study I, the method used to calculate EGP gave in some cases negative values in the experiments performed during euglycemic hyperinsulinemia. Since negative values are not physiological, we considered these negative values to be representing the cases with the highest suppression of EGP from insulin. It follows that even though the method that we have used for the calculation of EGP is validated against the gold standard of D-[6,6-^{2}H] glucose, it is not as precise as the gold standard.

In study II, we chose to examine whether there is any association between BGU and the parameters of ß-cell function in a dataset where we pooled data from smaller studies in which the timing of brain radioactivity acquisition varied. We applied a generally accepted statistical method to account for this discrepancy in the data by accounting for the time interval from [^{18}F]FDG injection to the brain scan. However, whether this statistical correction truly accounts for the difference in BGU when measured immediately after [^{18}F]FDG injection or later, is beyond the scope of our study.

Another important limitation of the current work is that the hypothalamus, a brain region of specific interest could not be adequately studied. The hypothalamus is a very small brain region and because of the physics of PET, minuscule anatomical regions cannot be analyzed with sufficient resolution (Teräs 2008).

Furthermore, in study III, we only used MRI to probe central nervous system inflammation. Though the analysis was performed by two independent neuroradiologists, with good agreement values between them, the results indicate that MRI may not be the optimal technique to detect brain inflammation.

In this study, only women were studied because of the fact that, in general, more women undergo bariatric surgery in Finland than men. Keeping the gender bias in mind, the results regarding brain fatty acid uptake should be generalized to men with caution, even though, the previous study by Karmi *et al.* reported similar BFAU rates also in men (Karmi et al., 2010).

6.2 Clinical implications and future perspectives

These studies deepen our knowledge of the pathophysiology of insulin resistance and the alterations that occur in the body and specifically in the brain with obesity/insulin resistance a bit more. We have shown that in the context of insulin resistance, there is increased substrate uptake from the brain (both glucose and free fatty acids). BGU correlates with both the determinants of glucose tolerance, i.e. endogenous glucose production, and insulin secretion, and these correlations occur independently of BMI and insulin sensitivity, respectively. BFAU also correlates with insulin secretion. Moreover, a higher brain substrate uptake at baseline predicts worse glycemic control at follow-up after bariatric surgery.

To better understand these results, we need to consider the term "central insulin resistance", which has been coined previously by other study groups. Whereas the definition of systemic insulin resistance is based on tissue-level studies where several molecular defects have been established, the characterization of human brain metabolism relies on different *in vivo* neuroimaging methods, such as PET, fMRI, and MEG. Accordingly, other study groups have thus far defined brain insulin resistance as a blunted cerebrocortical insulin effect when MEG is applied (Tschritter et al., 2012) or as a decreased intranasal insulin-induced suppression of hypothalamic blood flow in fMRI (Kullmann et al., 2020). Along with these definitions, we think that the increased substrate uptake in brain PET studies could be considered as another aspect of brain insulin resistance. In any case, the results of the current thesis show brain insulin misresponse in the context of systemic insulin resistance. Unfortunately, multiple neuroimaging measures are seldom used within a single study, and in the absence of a ground truth measurement of brain insulin resistance, the integration of our PET results with the fMRI and MEG results of others is complicated. Thus, it would be important to assess the consistency of these measures (MEG, fMRI and [^{18}F]FDG-PET) when applied to the same pool of subjects in order to reach a consensus on the definition of brain insulin resistance. This would be an important step in the better interpretation and understanding of this data.

In this context, whereas it is now well established that brain substrate uptake is increased in case of obesity/insulin resistance, it is not known whether "brain insulin resistance" occurs earlier, later, or at the same time with systemic insulin resistance

(the chicken and the egg problem). Our centre has also tried to clarify this by studying young subjects at risk of obesity. The results should be available shortly.

Moreover, based on the work for the current thesis, we have designed a new PET study, which addresses the question whether there is brain inflammation in the obese. If brain inflammation, in fact, is present, the need for a specific treatment – additional to the obvious and necessary treatments targeting weight loss – should be addressed.

Another valid hypothesis regarding the reason for increased BGU in subjects with obesity/insulin resistance is BBB leakage. More specifically, inflammation, hyperglycemia, and obesity have all been described to disrupt the BBB (Hargrave et al., 2016; Shah et al., 2013). The endothelium cells and the astrocytes express the GLUT-1 transporter, and in the presence of a normally functional BBB, glucose transport into the brain would occur mainly through them. However, in an altered/disrupted BBB, plasma glucose would reach the CNS also through these "cracks" in the BBB, and thus neurons would be exposed to higher glucose levels, which, in turn, could put stress on the redox balance of the neurons. In the future, it would be, thus, interesting to study whether the increased BGU in obese/insulin resistant subjects is to be attributed to an increased BBB permeability with either [^{18}F]FDG and a tracer that can be used to examine the permeability of the BBB (for instance the [^{68}Ga]DTPA has been proposed) (Breuer et al., 2017) or with [^{18}F]FDG and MRI with gadolinium (Breuer et al., 2017).

Finally, whether this increased substrate uptake in the brain is also linked to any early cognitive impairment has not been thus far elucidated, and this is an aspect that we are currently also exploring.

Even though the current results are probably still too distant from direct implementation in a clinical setup or clear new recommendations, the combination of these results and the new described information that should be available shortly (i.e. is there brain inflammation in human obesity, when does brain insulin resistance occur in the natural history of insulin resistance, is brain insulin resistance linked with cognitive dysfunction and worse metabolic outcome in the future) will hopefully help in developing novel ideas to be studied and ultimately may lead to new treatments in the battle against obesity.

7 Conclusions

I. Insulin-stimulated brain glucose uptake is increased in the obese subjects compared to lean individuals and is positively associated with endogenous glucose production, markers of systemic inflammation, and levels of branched-chain and aromatic amino acids, and it also predicts plasma glucose levels at follow-up. These results suggest that the enhanced brain glucose uptake in obese subjects might not only be an epiphenomenon, but also part of the pathophysiology that leads to further deterioration in metabolic diseases.

II. In subjects not affected by type 2 diabetes insulin-stimulated brain glucose uptake correlates positively with basal insulin secretion rate, total insulin output, and potentiation. In subjects affected by type 2 diabetes this pattern is altered since brain glucose uptake and insulin secretion do not correlate, but subjects with type 2 diabetes exhibit a clear negative correlation between BGU and potentiation. Brain fatty acid uptake also correlated differently with potentiation (negative correlation) and basal insulin secretion rate (positive correlation). Fasting BGU did not correlate with BISR. These results suggest that only in conditions where brain substrate uptake is increased in insulin resistance (insulin-stimulated state regarding BGU, and fasting state for BFAU), brain substrate uptake correlates with the parameters of β-cell function and that these correlations depend on the glucose tolerance status of the examined subjects. Even though correlations do not show cause-effect, these data suggest that also in humans the brain may be involved in the control of insulin secretion.

III. Brain fatty acid uptake is increased in morbidly obese women compared to lean women; and six months after bariatric surgery, BFAU remains increased. Contrary to our hypothesis, BFAU did not correlate with the hypothalamus/amygdala signal ratio, which has been described to depict hypothalamic inflammation. However, better techniques are needed in order to address whether brain inflammation occurs in human obesity. Finally, brain fatty acid uptake at baseline predicts worse glycemic control at two years of follow-up.

8 Acknowledgements

Because scripta manent verba volant…

This study was carried out at the Turku PET Centre, University of Turku, and Turku University Hospital. It was financially supported by the European Union as well as by grants from Academy of Finland, Diabetes Research Foundation, Turku University Hospital, Turku University Foundation, and Doctoral Programme of Clinical Research, University of Turku.

I express my appreciation to the Director of Turku PET Centre Professor Juhani Knuuti and to the Adjunct Professor Jukka Kemppainen from the Department of Clinical Physiology and Isotope Medicine for providing excellent research facilities.

I wish to express my gratitude to my supervisors Professor Pirjo Nuutila, Professor Ele Ferrannini, and Docent Riikka Lautamäki. Pirjo has been a great supervisor for me, she has always been supportive and giving me a lot of space to "cultivate" my research hypotheses and autonomy in performing clinical studies. She has never doubted me – at least not in plain sight –, and even during a period when I was practically not speaking any Finnish at all, she supported my participation in the studies, and for this I am grateful. I was not "research-naïve" when I came to Finland, but my experience here has definitely made me more of an independent researcher, and Pirjo's support in this process has been fundamental. After these three and a half years, during which we have worked actively together, I think we have built a nice professional but also friendly relationship. Ele Ferrannini is a person to whom I owe a lot. We first met 10 years ago, and he has taught me almost everything I know. I still remember the long afternoons/evenings in his office showing me how to analyze data. I was very young back then, knowing very little – if any – of statistics, and I still regret I did not have any hidden recorder on me, so that I could register those precious teachings. Apart from statistics, Professor Ferrannini really taught how to interpret the data, how to write an academic article, how to conduct metabolic studies, and eventually how to think as a researcher. Ultimately, he paved for me the way to accomplish a wish I had as a medical student which was to work one day as a researcher. I for sure had one of those professional experiences that only few young researchers ever get, and for which I am grateful. Riikka Lautamäki is my third

supervisor. I got to know Riikka very little (my PhD plan was initially on another topic, to which Riikka would have been for sure a great supervisor), but it changed to be related to brain metabolism. Still, in those few meetings, and other occasions that we had, I had the chance to appreciate her as a person and a researcher, and would just like to thank her for her help in getting my PhD completed. In this context, I should also mention my Endocrinology Professor at the University of Patras. Through her teachings Venetsana Kyriazopoulou inspired in me a love for endocrinology, and she was also the one who proposed me to Ele, after my graduation for six months of training at Pisa University under his supervision. That is where my journey started.

In addition to my supervisors, there are still many persons that need to be acknowledged. Docent Marco Bucci has been the person with whom I worked closely for three years. He taught me a lot about brain modeling and how to analyze brain data. Professor Lauri Nummenmaa has also been of great help for me during all these years, and I have enjoyed most of our discussions. There were some others where my intellect probably was not good enough to completely follow him. Docent Jarna Hannukainen has been a very positive person to work with, knowing many practical things regarding PET studies and always eager to help me. Docent Patricia Iozzo is also to be acknowledged. Even though I started from Pisa, I knew her back then mainly by her fame. I am glad I was given the possibility in Turku to work with her. Her advice was excellent and her expertise in metabolic studies using PET helped me a lot. Another Italian that should be acknowledged is the Engineer Andrea Mari who has been fundamental for the II study of this thesis and has patiently discussed several times with me about the difficult topics of insulin secretion and insulin clearance. Insisting on thanking Italian researchers, I also wish to thank Adjunct Professor Monica Nannipieri with whom I have worked closely on “bariatric” subjects during my residency years. Even though she was not involved in the present thesis, i am glad we have maintained a nice personal and professional relationship over the years. Adjunct Professor Jussi Hirvonen has been of great help. I thank him for his expertise and patience in analyzing (and re-analysing) those FLAIR images. Professor Juha Rinne, an active member of my follow-up committee, has also given me many useful pieces of advice, not just for my PhD, but also for the currently ongoing BARIBRAIN study. Adjunct Professor Paulina Salminen has been fundamental for the bariatric surgery interventions, collection of data and always with significant contribution to the manuscripts. Special thanks should also be given to Vesa Oikonen (our modeling guru); he has always been super helpful with modeling questions and other whatever type of questions I had. My personal opinion is that it is a pity Vesa is not a “Professor”, but if such a petition comes someday in the future, I would for sure support it! Professor Hidehiro Iida has given me many challenging questions and solutions on the difficult topic of renal PET imaging. His broad knowledge about brain imaging also helped us design the ongoing BARIBRAIN study.

Docent Sergey Nesterov is also to be acknowledged for the interesting discussions we have had during his lectures and generally. I give my sincere thanks to Sauli Pirola, Timo Laitinen, Rami Mikkola and Marco Tättäläinen for providing the IT and Carimas support. Especially Sauli has been of big help (and very patient) and helped us a lot with the kidney PET analyses. I would also like to thank Kalle Koskensalo for doing together the BARIBRAIN study, and Mika Teräs, Tuula Tolvanen, Virva Saunavaara and Jarmo Teuho our physicists, for their advice and help. Many thanks also to Lenita Saloranta for her help and her always friendly attitude.

I would really like to acknowledge my friends and colleagues from the PET Centre. Firstly, I would like to thank Miikka Honka, my roommate at the office. He was given the unique opportunity to support me almost every day during these three and a half years. He also got the opportunity to practice some Italian and Greek words (probably not the most recommended ones to use in everyday language) and also to support my mood. All in all, Miikka has been a great mate for discussions, gaming, gym, mushroom-picking, and last but not least a great colleague. Mueez U Din, Minna Lahesmaa and Prince Dadson are three other persons with whom I used to pass most of my time during the first two years of my PhD, but unfortunately after their dissertations we have split and ended up in different places. I have enjoyed their company and our discussions very much. Out of the still present friends and colleagues in Turku, I would like to thank Sanna Laurila, a very nice person (generally) and an excellent colleague. It has been very nice and relaxing working with her. Laura Pekkarinen has also been a very good colleague with whom I have enjoyed working with. With her help, we made it possible to clamp while performing MRI studies, a task that is more difficult than what one may think. Several more people need to be acknowledged: Adjunct Professor Kirsi Virtanen, Heidi Immonen, Aino Latva-Rasku, Susanne Vainio, Tomi Karjalainen, Jouni Tuisku, Ekaterina Saukko, Milena Monfort Pires, Luis Eduardo Juárez-Orozco, Olli Moisio, Marja Heiskanen, Ronja Ojala, Sanna Honkala, Priyanka Motiani, Kumail Motiani, Teemu Saari, Kerttu Seppälä, Lihua Sun, Vesa Putkinen, Janne Isojärvi, Sanaz Nazari, Tuulia Malén, Tanja Sjöros, Laura Ekblad, Anniina Snellman, and my friends Simona Malaspina, Mia Ståhle, Riikka Siitonen, and Janne Verho are all people I had the opportunity to appreciate – each for a different reason – during these years. Docent Kaisa Ivaska-Papaioannou helped me a lot in my struggle with the Finnish language and I have enjoyed our “literal” coffees.

I would also like to thank our study nurse Sanna Himanen. I have worked with Sanna since the first day she arrived at the PET Centre almost on a daily basis. I thank Sanna because without her DAPACARD and BARIBRAIN would have been impossible to perform, and I think that we have made a nice team. Many other “lab subjects” need to be addressed, and especially I give many thanks to Sanna Suominen, Eija Salo, Heidi Partanen, Minna Aatsinki and my personal favorite

"anesthesiologist" Anne-Marie Jokinen. They have all been super helpful in the studies, and we have also had a nice time.

Finally, I would also like to give my warm thank you to the two reviewers of my thesis Associate Professor Vera Schrauwen-Hinderling and Professor Riccardo Bonadonna, who through their constructive criticism and their expert comments have definitely improved the quality of my thesis. Jussi Heinonen, M.A., LL.B., is also to be acknowledged for the careful language editing of the present thesis. I would also like to thank Professor Mikael Rydén for accepting the invitation to become my opponent and I am looking forward for our discussion.

Regarding my personal life, it comes without saying that I owe the biggest thank you to my family. We are a typical Greek family, and what I mean by that, is that its members support each other. Through hard and easy times my family has always been my κολώνα and I know that we have been the κολώνες of each other. There are many small things I could discuss about my family, but what I would like to write here is actually a small story about my grandfather. My grandfather, a Professor of Physics in High-school, who reached the highest step in a teacher's carrier, was the first person to study at the University from his (my) village. He was always admired and loved by the locals. Apart from the influence my grandpa directly had on me, I always remember a phrase my father used to tell me when I was "naughty" as a kid. He would say to me: "*do you know whom you have for a grandfather?"* Even though my grandpa was neither a Greek prime minister, nor any other famous person, this phrase meant the world to me, and since then I have always been trying to achieve something in my life. Even though I am still in this process, I consider it as one of those things that really affected my way of being.

I would also like to thank some very good friends Natasa, Kostas, Vaggelitsa, my good Greek friends; we have shared a friendship of many years and even though I have lived abroad for over a decade now, they always manage to make me feel just like home when we meet. My good friends from my University years Konstantina, Katerina, Poly, Vasileia, Sakis, Tasos, Kostas Pittas, Kostas Papatheodorou, Giorgos, and Kleanthis are people with whom I hope our friendship will last forever. My few good Italian friends Renzo, Silvia, and Alessia are also to be mentioned. I am really looking forward to meeting them again, now that this PhD will be completed, and my future will probably bring me back to Pisa. Last but not least, I would like to thank Nicolò. Nicolò does not need to be introduced to most of the readers of these pages. He has been my support for many years now. I thank him for all these years of caring that he has selflessly given me.

Turku, July 2020
Eleni Rebelos

9 References

Alonso-Nanclares L, Gonzalez-Soriano J, Rodriguez JR, DeFelipe J. 2008. Gender differences in human cortical synaptic density. *Proceedings of the National Academy of Sciences of the United States of America* 105:14615–14619.

Astiarraga B, Chueire VB, Souza AL, Pereira-Moreira R, Monte Alegre S, Natali A, Tura A, Mari A, Ferrannini E, Muscelli E. 2018. Effects of acute nefa manipulation on incretin-induced insulin secretion in participants with and without type 2 diabetes. *Diabetologia* 61:1829–1837.

Bahri S, Horowitz M, Malbert CH. 2018. Inward glucose transfer accounts for insulin-dependent increase in brain glucose metabolism associated with diet-induced obesity. *Obesity (Silver Spring)* 26:1322–1331.

Baker LD, Cross DJ, Minoshima S, Belongia D, Watson GS, Craft S. 2011. Insulin resistance and alzheimer-like reductions in regional cerebral glucose metabolism for cognitively normal adults with prediabetes or early type 2 diabetes. *Archives of neurology* 68:51–57.

Banks WA, Jaspan JB, Kastin AJ. 1997. Selective, physiological transport of insulin across the blood-brain barrier: Novel demonstration by species-specific radioimmunoassays. *Peptides* 18:1257–1262.

Baroncini M, Jissendi P, Catteau-Jonard S, Dewailly D, Pruvo JP, Francke JP, Prevot V. 2010. Sex steroid hormones-related structural plasticity in the human hypothalamus. *NeuroImage* 50:428–433.

Benedict C, Brede S, Schioth HB, Lehnert H, Schultes B, Born J, Hallschmid M. 2011. Intranasal insulin enhances postprandial thermogenesis and lowers postprandial serum insulin levels in healthy men. *Diabetes* 60:114–118.

Bingham EM, Hopkins D, Smith D, Pernet A, Hallett W, Reed L, Marsden PK, Amiel SA. 2002. The role of insulin in human brain glucose metabolism: An 18fluoro-deoxyglucose positron emission tomography study. *Diabetes* 51:3384–3390.

Bishop J, Simpkins JW. 1992. Role of estrogens in peripheral and cerebral glucose utilization. *Reviews in the neurosciences* 3:121–138.

Breuer H, Meier M, Schneefeld S, Härtig W, Wittneben A, Märkel M, Ross TL, Bengel FM, Bankstahl M, Bankstahl JP. 2017. Multimodality imaging of blood-brain barrier impairment during epileptogenesis. *Journal of cerebral blood flow and metabolism: official journal of the International Society of Cerebral Blood Flow and Metabolism* 37:2049–2061.

Brownell KD, Rodin J. 1994. Medical, metabolic, and psychological effects of weight cycling. *Archives of internal medicine* 154:1325–1330.

Bruning JC, Gautam D, Burks DJ, Gillette J, Schubert M, Orban PC, Klein R, Krone W, Muller-Wieland D, Kahn CR. 2000. Role of brain insulin receptor in control of body weight and reproduction. Science (New York, NY). 289:2122–2125.

Camandola S. 2018. Astrocytes, emerging stars of energy homeostasis. *Cell stress* 2:246–252.

Camastra S, Manco M, Mari A, Baldi S, Gastaldelli A, Greco AV, Mingrone G, Ferrannini E. 2005. Beta-cell function in morbidly obese subjects during free living: Long-term effects of weight loss. *Diabetes* 54:2382–2389.

Chowen JA, Argente-Arizon P, Freire-Regatillo A, Argente J. 2018. Sex differences in the neuroendocrine control of metabolism and the implication of astrocytes. *Frontiers in neuroendocrinology* 48:3–12.

Craft S, Baker LD, Montine TJ, Minoshima S, Watson GS, Claxton A, Arbuckle M, Callaghan M, Tsai E, Plymate SR et al. 2012. Intranasal insulin therapy for alzheimer disease and amnestic mild cognitive impairment: A pilot clinical trial. *Archives of neurology* 69:29–38.

Cruciani-Guglielmacci C, Hervalet A, Douared L, Sanders NM, Levin BE, Ktorza A, Magnan C. 2004. Beta oxidation in the brain is required for the effects of non-esterified fatty acids on glucose-induced insulin secretion in rats. *Diabetologia*. 47:2032–2038.

Dadson P, Ferrannini E, Landini L, Hannukainen JC, Kalliokoski KK, Vaittinen M, Honka H, Karlsson HK, Tuulari JJ, Soinio M et al. 2017. Fatty acid uptake and blood flow in adipose tissue compartments of morbidly obese subjects with or without type 2 diabetes: Effects of bariatric surgery. *American journal of physiology Endocrinology and metabolism*. 313:E175–e182.

de Graaf RA. 2018. In vivo nmr spectroscopy: Principles and techniques. Chichester: Wiley.

DeFronzo RA, Tobin JD, Andres R. 1979. Glucose clamp technique: A method for quantifying insulin secretion and resistance. *The American journal of physiology* 237:E214–223.

Del Prato S, Leonetti F, Simonson DC, Sheehan P, Matsuda M, DeFronzo RA. 1994. Effect of sustained physiologic hyperinsulinaemia and hyperglycaemia on insulin secretion and insulin sensitivity in man. *Diabetologia* 37:1025–1035.

Dezonne RS, Lima FR, Trentin AG, Gomes FC. 2015. Thyroid hormone and astroglia: Endocrine control of the neural environment. *Journal of neuroendocrinology* 27:435–445.

Diamond MC, Scheibel AB, Murphy GM, Jr., Harvey T. 1985. On the brain of a scientist: Albert einstein. *Experimental neurology* 88:198–204.

Diano S, Kalra SP, Horvath TL. 1998. Leptin receptor immunoreactivity is associated with the golgi apparatus of hypothalamic neurons and glial cells. *Journal of neuroendocrinology* 10:647–650.

Diaz-Garcia CM, Mongeon R, Lahmann C, Koveal D, Zucker H, Yellen G. 2017. Neuronal stimulation triggers neuronal glycolysis and not lactate uptake. *Cell metabolism* 26:361–374.e364.

Dietz WH, Jr., Gortmaker SL. 1985. Do we fatten our children at the television set? Obesity and television viewing in children and adolescents. *Pediatrics* 75:807–812.

Edmond J. 1992. Energy metabolism in developing brain cells. *Canadian journal of physiology and pharmacology* 70 Suppl:S118–129.

Edmond J, Robbins RA, Bergstrom JD, Cole RA, de Vellis J. 1987. Capacity for substrate utilization in oxidative metabolism by neurons, astrocytes, and oligodendrocytes from developing brain in primary culture. *Journal of neuroscience research* 18:551–561.

Falomir-Lockhart LJ, Cavazzutti GF, Gimenez E, Toscani AM. 2019. Fatty acid signaling mechanisms in neural cells: Fatty acid receptors. *Frontiers in cellular neuroscience* 13:162.

Fernandez AM, Torres-Aleman I. 2012. The many faces of insulin-like peptide signalling in the brain. *Nature reviews Neuroscience* 13:225–239.

Friede R. 1954. [quantitative share of the glia in development of the cortex]. *Acta anatomica* 20:290–296.

Fu W, Patel A, Jhamandas JH. 2013. Amylin receptor: A common pathophysiological target in alzheimer's disease and diabetes mellitus. *Frontiers in aging neuroscience* 5:42.

Fuente-Martin E, Garcia-Caceres C, Argente-Arizon P, Diaz F, Granado M, Freire-Regatillo A, Castro-Gonzalez D, Ceballos ML, Frago LM, Dickson SL et al. 2016. Ghrelin regulates glucose and glutamate transporters in hypothalamic astrocytes. *Scientific reports* 6:23673.

Gancheva S, Koliaki C, Bierwagen A, Nowotny P, Heni M, Fritsche A, Haring HU, Szendroedi J, Roden M. 2015. Effects of intranasal insulin on hepatic fat accumulation and energy metabolism in humans. *Diabetes* 64:1966–1975.

Garcia-Caceres C, Quarta C, Varela L, Gao Y, Gruber T, Legutko B, Jastroch M, Johansson P, Ninkovic J, Yi CX et al. 2016. Astrocytic insulin signaling couples brain glucose uptake with nutrient availability. *Cell* 166:867–880.

Garcia-Ovejero D, Azcoitia I, Doncarlos LL, Melcangi RC, Garcia-Segura LM. 2005. Glia-neuron crosstalk in the neuroprotective mechanisms of sex steroid hormones. *Brain research reviews* 48:273–286.

Garcia-Segura LM, Cardona-Gomez GP, Chowen JA, Azcoitia I. 2000. Insulin-like growth factor-i receptors and estrogen receptors interact in the promotion of neuronal survival and neuroprotection. *Journal of neurocytology* 29:425–437.

Goyal MS, Vlassenko AG, Blazey TM, Su Y, Couture LE, Durbin TJ, Bateman RJ, Benzinger TL, Morris JC, Raichle ME. 2017. Loss of brain aerobic glycolysis in normal human aging. *Cell metabolism* 26:353–360.e353.

Guillod-Maximin E, Lorsignol A, Alquier T, Penicaud L. 2004. Acute intracarotid glucose injection towards the brain induces specific c-fos activation in hypothalamic nuclei: Involvement of astrocytes in cerebral glucose-sensing in rats. *Journal of neuroendocrinology* 16:464–471.

Hamacher K, Coenen HH, Stocklin G. 1986. Efficient stereospecific synthesis of no-carrier-added 2-[18f]-fluoro-2-deoxy-d-glucose using aminopolyether supported nucleophilic substitution. Journal of nuclear medicine : official publication, *Society of Nuclear Medicine* 27:235–238.

Hamilton JA, Hillard CJ, Spector AA, Watkins PA. 2007. Brain uptake and utilization of fatty acids, lipids and lipoproteins: Application to neurological disorders. *Journal of molecular neuroscience : MN* 33:2–11.

Hannukainen JC, Lautamaki R, Parkka J, Strandberg M, Saunavaara V, Hurme S, Soinio M, Dadson P, Virtanen KA, Gronroos T et al. 2018. Reversibility of myocardial metabolism and remodeling in morbidly obese patients 6 months after bariatric surgery. *Diabetes, obesity & metabolism* 20:963–973.

Hargrave SL, Davidson TL, Zheng W, Kinzig KP. 2016. Western diets induce blood-brain barrier leakage and alter spatial strategies in rats. *Behavioral neuroscience* 130:123–135.

Heni M, Wagner R, Kullmann S, Gancheva S, Roden M, Peter A, Stefan N, Preissl H, Haring HU, Fritsche A. 2017. Hypothalamic and striatal insulin action suppresses endogenous glucose production and may stimulate glucose uptake during hyperinsulinemia in lean but not in overweight men. *Diabetes* 66:1797-1806.

Hirvonen J, Virtanen KA, Nummenmaa L, Hannukainen JC, Honka MJ, Bucci M, Nesterov SV, Parkkola R, Rinne J, Iozzo P, et al. 2011. Effects of insulin on brain glucose metabolism in impaired glucose tolerance. *Diabetes* 60:443–447.

Ho AJ, Raji CA, Becker JT, Lopez OL, Kuller LH, Hua X, Lee S, Hibar D, Dinov ID, Stein JL et al. 2010. Obesity is linked with lower brain volume in 700 ad and mci patients. *Neurobiology of aging* 31:1326–1339.

Hotamisligil GS. 2006. Inflammation and metabolic disorders. *Nature* 444:860–867.

Immonen H, Hannukainen JC, Kudomi N, Pihlajamäki J, Saunavaara V, Laine J, Salminen P, Lehtimäki T, Pham T, Iozzo P, Nuutila P. 2018. Increased liver fatty acid uptake is partly reversed and liver fat content normalized after bariatric surgery. *Diabetes Care* 41:368–371.

Inouye M, Kettunen J, Soininen P, Silander K, Ripatti S, Kumpula LS, Hamalainen E, Jousilahti P, Kangas AJ, Mannisto S et al. 2010. Metabonomic, transcriptomic, and genomic variation of a population cohort. *Molecular systems biology* 6:441.

Iozzo P, Gastaldelli A, Jarvisalo MJ, Kiss J, Borra R, Buzzigoli E, Viljanen A, Naum G, Viljanen T, Oikonen V et al. 2006. 18f-fdg assessment of glucose disposal and production rates during fasting and insulin stimulation: A validation study. *Journal of nuclear medicine : official publication, Society of Nuclear Medicine* 47:1016–1022.

Iozzo P, Turpeinen AK, Takala T, Oikonen V, Solin O, Ferrannini E, Nuutila P, Knuuti J. 2003. Liver uptake of free fatty acids in vivo in humans as determined with 14(r, s)-[18f]fluoro-6-thia-heptadecanoic acid and pet. *European journal of nuclear medicine and molecular imaging* 30:1160–1164.

Kappeler L, De Magalhaes Filho C, Dupont J, Leneuve P, Cervera P, Perin L, Loudes C, Blaise A, Klein R, Epelbaum J et al. 2008. Brain igf-1 receptors control mammalian growth and lifespan through a neuroendocrine mechanism. *PLoS biology* 6:e254.

Karjalainen T, Tuisku J, Santavirta S, Kantonen T, Bucci M, Tuominen L, Hirvonen J, Hietala J, Rinne JO, Nummenmaa L. 2020. Magia: Robust Automated Image Processing and Kinetic Modeling Toolbox for PET Neuroinformatics. *Front Neuroinform* 4:14:3.

Karmi A, Iozzo P, Viljanen A, Hirvonen J, Fielding BA, Virtanen K, Oikonen V, Kemppainen J, Viljanen T, Guiducci L et al. 2010. Increased brain fatty acid uptake in metabolic syndrome. *Diabetes* 59:2171–2177.

Kelly T, Yang W, Chen CS, Reynolds K, He J. 2008. Global burden of obesity in 2005 and projections to 2030. *International journal of obesity (2005)* 32:1431–1437.

Kern W, Benedict C, Schultes B, Plohr F, Moser A, Born J, Fehm HL, Hallschmid M. 2006. Low cerebrospinal fluid insulin levels in obese humans. *Diabetologia* 49:2790–2792.

Kleinridders A, Lauritzen HP, Ussar S, Christensen JH, Mori MA, Bross P, Kahn CR. 2013. Leptin regulation of hsp60 impacts hypothalamic insulin signaling. *The Journal of clinical investigation* 123:4667–4680.

Kleinridders A, Schenten D, Konner AC, Belgardt BF, Mauer J, Okamura T, Wunderlich FT, Medzhitov R, Bruning JC. 2009. Myd88 signaling in the cns is required for development of fatty acid-induced leptin resistance and diet-induced obesity. *Cell metabolism* 10:249–259.

Kreutzer C, Peters S, Schulte DM, Fangmann D, Turk K, Wolff S, van Eimeren T, Ahrens M, Beckmann J, Schafmayer C et al. 2017. Hypothalamic inflammation in human obesity is mediated by environmental and genetic factors. *Diabetes* 66(9):2407–2415.

Kullmann S, Heni M, Veit R, Scheffler K, Machann J, Haring HU, Fritsche A, Preissl H. 2017. Intranasal insulin enhances brain functional connectivity mediating the relationship between adiposity and subjective feeling of hunger. *Scientific Reports* 7(1):1627.

Kullmann S, Kleinridders A, Small DM, Fritsche A, Häring HU, Preissl H, Heni M. 2020. Central nervous pathways of insulin action in the control of metabolism and food intake. *The Lancet Diabetes & endocrinology*. 8(6):524–534.

Lam TK, Pocai A, Gutierrez-Juarez R, Obici S, Bryan J, Aguilar-Bryan L, Schwartz GJ, Rossetti L. 2005. Hypothalamic sensing of circulating fatty acids is required for glucose homeostasis. *Nature medicine* 11(3):320–327.

Latva-Rasku A, Honka MJ, Stancakova A, Koistinen HA, Kuusisto J, Guan L, Manning AK, Stringham H, Gloyn AL, Lindgren CM et al. 2018. A partial loss-of-function variant in akt2 is associated with reduced insulin-mediated glucose uptake in multiple insulin sensitive tissues: A genotype-based callback positron emission tomography study. *Diabetes* 67:334-342.

Le Foll C, Dunn-Meynell AA, Miziorko HM, Levin BE. 2014. Regulation of hypothalamic neuronal sensing and food intake by ketone bodies and fatty acids. *Diabetes* 63:1259–1269.

Le Foll C, Irani BG, Magnan C, Dunn-Meynell AA, Le*vin BE. 2009. Characteristics and mechanisms of hypothalamic neuronal fatty acid sensing. American journal of physiology Regulatory, integrative and comparative physiology* 297:R655–664.

Lee J, Kim K, Cho JH, Bae JY, O'Leary TP, Johnson JD, Bae YC, Kim EK. 2020. Insulin synthesized in the paraventricular nucleus of the hypothalamus regulates pituitary growth hormone production. *JCI insight.*

Magnan C, Collins S, Berthault MF, Kassis N, Vincent M, Gilbert M, Penicaud L, Ktorza A, Assimacopoulos-Jeannet F. 1999. Lipid infusion lowers sympathetic nervous activity and leads to increased beta-cell responsiveness to glucose. *The Journal of clinical investigation* 103(3):413–419.

Mari A, Ferrannini E. 2008. Beta-cell function assessment from modeling of oral tests: An effective approach. *Diabetes, obesity & metabolism* 10 Suppl 4:77–87.

Mari A, Schmitz O, Gastaldelli A, Oestergaard T, Nyholm B, Ferrannini E. 2002a. Meal and oral glucose tests for assessment of beta -cell function: Modeling analysis in normal subjects. *American journal of physiology Endocrinology and metabolism* 283:E1159–1166.

Mari A, Tura A, Gastaldelli A, Ferrannini E. 2002b. Assessing insulin secretion by modeling in multiple-meal tests: Role of potentiation. *Diabetes* 51 Suppl 1:S221–226.

Marks DR, Tucker K, Cavallin MA, Mast TG, Fadool DA. 2009. Awake intranasal insulin delivery modifies protein complexes and alters memory, anxiety, and olfactory behaviors. *The Journal of neuroscience : the official journal of the Society for Neuroscience* 29:6734–6751.

Marty N, Dallaporta M, Foretz M, Emery M, Tarussio D, Bady I, Binnert C, Beermann F, Thorens B. 2005. Regulation of glucagon secretion by glucose transporter type 2 (glut2) and astrocyte-dependent glucose sensors. *The Journal of clinical investigation* 115:3545–3553.

Marty N, Dallaporta M, Thorens B. 2007. Brain glucose sensing, counterregulation, and energy homeostasis. *Physiology (Bethesda, Md)* 22:241–251.

Michaelson DM. 2014. Apoe epsilon4: The most prevalent yet understudied risk factor for alzheimer's disease. *Alzheimer's & dementia : the journal of the Alzheimer's Association* 10:861–868.

Mink JW, Blumenschine RJ, Adams DB. 1981. Ratio of central nervous system to body metabolism in vertebrates: Its constancy and functional basis. *The American journal of physiology* 241:R203–212.

Mokdad AH, Ford ES, Bowman BA, Dietz WH, Vinicor F, Bales VS., Marks JS. 2003. Prevalence of obesity, diabetes, and obesity-related health risk factors, 2001. *Jama* 289:76–79.

Mong JA, Glaser E, McCarthy MM. 1999. Gonadal steroids promote glial differentiation and alter neuronal morphology in the developing hypothalamus in a regionally specific manner. *The Journal of neuroscience : the official journal of the Society for Neuroscience* 19:1464–1472.

Moriconi D, Masi S, Rebelos E, Virdis A, Manca ML, De Marco S, Taddei S, Nannipieri M. 2020. Obesity prolongs the hospital stay in patients affected by covid-19, and may impact on sars-cov-2 shedding. *Obesity research & clinical practice* 14:205–209.

Munzberg H, Flier JS, Bjorbaek C. 2004. Region-specific leptin resistance within the hypothalamus of diet-induced obese mice. *Endocrinology* 145:4880–4889.

Namba H, Sokoloff L. 1984. Acute administration of high doses of estrogen increases glucose utilization throughout brain. *Brain research* 291:391–394.

Nguyen DM, El-Serag HB. 2010. The epidemiology of obesity. *Gastroenterology clinics of North America* 39(1):1–7.

Obici S, Zhang BB, Karkanias G, Rossetti L. 2002a. Hypothalamic insulin signaling is required for inhibition of glucose production. *Nature Medicine* 8:1376-82.

Obici S, Feng Z, Morgan K, Stein D, Karkanias G, Rossetti L. 2002b. Central administration of oleic acid inhibits glucose production and food intake. *Diabetes* 51:271–275.

Okamoto H, Obici S, Accili D, Rossetti L. 2005. Restoration of liver insulin signaling in insr knockout mice fails to normalize hepatic insulin action. *The Journal of clinical investigation* 115:1314–1322.

Oomura Y, Kimura K, Ooyama H, Maeno T, Iki M, Kuniyoshi M. 1964. Reciprocal activities of the ventromedial and lateral hypothalamic areas of cats. *Science (New York, NY)* 143(3605):484–485.

Oomura Y, Kita H. 1981. Insulin acting as a modulator of feeding through the hypothalamus. *Diabetologia* 20 Suppl:290–298.

Ott A, Stolk RP, van Harskamp F, Pols HA, Hofman A, Breteler MM. 1999. Diabetes mellitus and the risk of dementia: The rotterdam study. *Neurology* 53:1937–1942.

Owen OE, Morgan AP, Kemp HG, Sullivan JM, Herrera MG, Cahill GF, Jr. 1967. Brain metabolism during fasting. *The Journal of clinical investigation* 46:1589–1595.

Pakkenberg B, Gundersen HJ. 1997. Neocortical neuron number in humans: Effect of sex and age. *The Journal of comparative neurology* 384:312–320.

Patlak CS, Blasberg RG. 1985. Graphical evaluation of blood-to-brain transfer constants from multiple-time uptake data. Generalizations. *Journal of cerebral blood flow and metabolism : official journal of the International Society of Cerebral Blood Flow and Metabolism* 5:584–590.

Pellerin L, Magistretti PJ. 1994. Glutamate uptake into astrocytes stimulates aerobic glycolysis: A mechanism coupling neuronal activity to glucose utilization. *Proceedings of the National Academy of Sciences of the United States of America* 91:10625–10629.

Pelvig DP, Pakkenberg H, Stark AK, Pakkenberg B. 2008. Neocortical glial cell numbers in human brains. *Neurobiology of aging* 29:1754–1762.

Pocai A, Lam TKT, Gutierrez-Juarez R, Obici S, Schwartz GJ, Bryan J, Aguilar-Bryan L, Rossetti L.

2005. Hypothalamic KATP channels control hepatic glucose production. *Nature* 434:1026-1031.

Prada PO, Zecchin HG, Gasparetti AL, Torsoni MA, Ueno M, Hirata AE, Corezola do Amaral ME, Hoer NF, Boschero AC, Saad MJ. 2005. Western diet modulates insulin signaling, c-jun n-terminal kinase activity, and insulin receptor substrate-1ser307 phosphorylation in a tissue-specific fashion. *Endocrinology* 146:1576–1587.

Profenno LA, Porsteinsson AP, Faraone SV. 2010. Meta-analysis of alzheimer's disease risk with obesity, diabetes, and related disorders. *Biological psychiatry* 67:505–512.

Pugazhenthi S, Qin L, Reddy PH. 2017. Common neurodegenerative pathways in obesity, diabetes, and alzheimer's disease. *Biochimica et biophysica acta Molecular basis of disease* 1863:1037–1045.

Puzziferri N, Roshek TB, 3rd, Mayo HG, Gallagher R, Belle SH, Livingston EH. 2014. Long-term follow-up after bariatric surgery: A systematic review. *Jama* 312:934–942.

Rapoport SI, Chang MC, Spector AA. 2001. Delivery and turnover of plasma-derived essential pufas in mammalian brain. *Journal of lipid research* 42:678–685.

Rebelos E, Astiarraga B, Bizzotto R, Mari A, Manca ML, Gonzalez A, Mendez A, Martinez CA, Hurwitz BE, Ferrannini E. 2017. Glp-1 response to sequential mixed meals: Influence of insulin resistance. *Clinical science (London, England : 1979)* 131:2901–2910.

Rebelos E, Dadson P, Oikonen V, Iida H, Hannukainen JC, Iozzo P, Ferrannini E, Nuutila P. 2019. Renal hemodynamics and fatty acid uptake: Effects of obesity and weight loss. *American journal of physiology Endocrinology and metabolism* 317:E871-878.

Rebelos E, Moriconi D, Scalese M, Denoth F, Molinaro S, Siciliano V, Anselmino M, Taddei S, Ferrannini E, Nannipieri M. 2020a. Impact of postprandial hypoglycemia on weight loss after bariatric surgery. *Obesity surgery* 30:2266–2273.

Rebelos E, Moriconi D, Virdis A, Taddei S, Foschi D, Nannipieri M. 2020b. Letter to the editor: Importance of metabolic health in the era of covid-19. *Metabolism: clinical and experimental* 108:154247.

Rebelos E, Seghieri M, Natali A, Balkau B, Golay A, Piatti PM, Lalic NM, Laakso M, Mari A, Ferrannini E. 2015. Influence of endogenous nefa on beta cell function in humans. *Diabetologia* 58:2344–2351.

Reiner DJ, Mietlicki-Baase EG, McGrath LE, Zimmer DJ, Bence KK, Sousa GL, Konanur VR, Krawczyk J. 2016. Astrocytes regulate glp-1 receptor-mediated effects on energy balance. *The journal of neuroscience* 36:3531–3540.

Sanchez-Alavez M, Osborn O, Tabarean IV, Holmberg KH, Eberwine J, Kahn CR, Bartfai T. 2011. Insulin-like growth factor 1-mediated hyperthermia involves anterior hypothalamic insulin receptors. *The Journal of biological chemistry* 286:14983–14990.

Schonfeld P, Reiser G. 2013. Why does brain metabolism not favor burning of fatty acids to provide energy? Reflections on disadvantages of the use of free fatty acids as fuel for brain. *Journal of cerebral blood flow and metabolism : official journal of the International Society of Cerebral Blood Flow and Metabolism* 33:1493–1499.

Schur EA, Melhorn SJ, Oh SK, Lacy JM, Berkseth KE, Guyenet SJ, Sonnen JA, Tyagi V, Rosalynn M, De Leon B et al. 2015. Radiologic evidence that hypothalamic gliosis is associated with obesity and insulin resistance in humans. *Obesity (Silver Spring, Md)* 23:2142–2148.

Seaquist ER, Anderson J, Childs B, Cryer P, Dagogo-Jack S, Fish L, Heller SR, Rodriguez H, Rosenzweig J, Vigersky R. 2013. Hypoglycemia and diabetes: A report of a workgroup of the american diabetes association and the endocrine society. *Diabetes Care* 36:1384–1395.

Shah GN, Morofuji Y, Banks WA, Price TO. 2013. High glucose-induced mitochondrial respiration and reactive oxygen species in mouse cerebral pericytes is reversed by pharmacological inhibition of mitochondrial carbonic anhydrases: Implications for cerebral microvascular disease in diabetes. *Biochemical and biophysical research communications* 440:354–358.

Soininen P, Kangas AJ, Wurtz P, Suna T, Ala-Korpela M. 2015. Quantitative serum nuclear magnetic resonance metabolomics in cardiovascular epidemiology and genetics. *Circulation Cardiovascular genetics* 8:192–206.

Steen E, Terry BM, Rivera EJ, Cannon JL, Neely TR, Tavares R, Xu XJ, Wands JR, de la Monte SM. 2005. Impaired insulin and insulin-like growth factor expression and signaling mechanisms in alzheimer's disease--is this type 3 diabetes? *Journal of Alzheimer's disease : JAD* 7:63–80.

Takala TO, Nuutila P, Pulkki K, Oikonen V, Gronroos T, Savunen T, Vahasilta T, Luotolahti M, Kallajoki M, Bergman J et al. 2002. 14(r,s)-[18f]fluoro-6-thia-heptadecanoic acid as a tracer of free fatty acid uptake and oxidation in myocardium and skeletal muscle. *European journal of nuclear medicine and molecular imaging* 29:1617–1622.

Teräs M. 2008. Performance and methodological aspects in positron emission tomography. Turku: Turun Yliopisto.

Thaler JP, Yi CX, Schur EA, Guyenet SJ, Hwang BH, Dietrich MO, Zhao X, Sarruf DA, Izgur V, Maravilla KR et al. 2012. Obesity is associated with hypothalamic injury in rodents and humans. *The Journal of clinical investigation* 122:153–162.

Trico D, Natali A, Arslanian S, Mari A, Ferrannini E. 2018. Identification, pathophysiology, and clinical implications of primary insulin hypersecretion in nondiabetic adults and adolescents. *JCI insight* 3:e124912.

Tschritter O, Preissl H, Hennige AM, Sartorius T, Stingl KT, Heni M, Ketterer C, Stefan N, Machann J, Schleicher E et al. 2012. High cerebral insulin sensitivity is associated with loss of body fat during lifestyle intervention. *Diabetologia* 55:175–182

Turku PET Centre, Oikonen V. 2019. Pet data analysis and modeling.

Tuulari JJ, Karlsson HK, Hirvonen J, Hannukainen JC, Bucci M, Helmio M, Ovaska J, Soinio M, Salminen P, Savisto N et al. 2013. Weight loss after bariatric surgery reverses insulin-induced increases in brain glucose metabolism of the morbidly obese. *Diabetes* 62:2747–2751.

Van Cauter E, Mestrez F, Sturis J, Polonsky KS. 1992. Estimation of insulin secretion rates from c-peptide levels. Comparison of individual and standard kinetic parameters for c-peptide clearance. *Diabetes* 41:368–377.

Vazquez G, Duval S, Jacobs DR, Jr., Silventoinen K. 2007. Comparison of body mass index, waist circumference, and waist/hip ratio in predicting incident diabetes: A meta-analysis. *Epidemiologic reviews* 29:115–128.

Velloso LA, Schwartz MW. 2011. Altered hypothalamic function in diet-induced obesity. *International journal of obesity (2005)* 35:1455–1465.

Vergnaud AC, Bertrais S, Oppert JM, Maillard-Teyssier L, Galan P, Hercberg S, Czernichow S. 2008. Weight fluctuations and risk for metabolic syndrome in an adult cohort. *International journal of obesity (2005)* 32:315–321.

Verkhratsky A BA. 2013. "Numbers: How many glial cells are in the brain?". *Glia physiology and pathophysiology*. Wiley-Blackwell.

Wang KC, Woung LC, Tsai MT, Liu CC, Su YH, Li CY. 2012. Risk of alzheimer's disease in relation to diabetes: A population-based cohort study. *Neuroepidemiology* 38:237–244.

Warnes GR, Bolker B, Bonebakker L, Gentleman R, Liaw WHA, Lumley T, Maechler M, Magnusson A, Moeller S, Schwartz M et al. 2016. Gplots: Various r programming tools for plotting data. R package version 3.0.1. CRAN.

Weindl A, Sofroniew MV. 1981. Relation of neuropeptides to mammalian circumventricular organs. *Advances in biochemical psychopharmacology* 28:303–320.

Weir JB. 1949. New methods for calculating metabolic rate with special reference to protein metabolism. *The Journal of physiology* 109:1–9.

Weiss EC, Galuska DA, Kettel Khan L, Gillespie C, Serdula MK. 2007. Weight regain in u.S. Adults who experienced substantial weight loss, 1999–2002. *American journal of preventive medicine* 33:34–40.

Weyer C, Hanson RL, Tataranni PA, Bogardus C, Pratley RE. 2000. A high fasting plasma insulin concentration predicts type 2 diabetes independent of insulin resistance: Evidence for a pathogenic role of relative hyperinsulinemia. *Diabetes* 49:2094–2101.

Whiting DR, Guariguata L, Weil C, Shaw J. 2011. Idf diabetes atlas: Global estimates of the prevalence of diabetes for 2011 and 2030. *Diabetes research and clinical practice* 94:311–321.

Williamson R, McNeilly A, Sutherland C. 2012. Insulin resistance in the brain: An old-age or new-age problem? *Biochemical pharmacology* 84:737–745.

Woods SC, Seeley RJ, Baskin DG, Schwartz MW. 2003. Insulin and the blood-brain barrier. *Current pharmaceutical design* 9:795–800.

World Health O. 2018. Obesity and overweight. Geneve: World Health Organization.

Wu HM, Bergsneider M, Glenn TC, Yeh E, Hovda DA, Phelps ME, Huang SC. 2003. Measurement of the global lumped constant for 2-deoxy-2-[18f]fluoro-d-glucose in normal human brain using [15o]water and 2-deoxy-2-[18f]fluoro-d-glucose positron emission tomography imaging. A method with validation based on multiple methodologies. *Molecular imaging and biology : MIB : the official publication of the Academy of Molecular Imaging* 5:32–41.

Zhao WQ, Chen H, Quon MJ, Alkon DL. 2004. Insulin and the insulin receptor in experimental models of learning and memory. *European journal of pharmacology* 490:71–81.

Zierler KL. 1961. Theory of the use of arteriovenous concentration differences for measuring metabolism in steady and non-steady states. *The Journal of clinical investigation* 40:2111–2125.

Zimmer ER, Parent MJ, Souza DG, Leuzy A, Lecrux C, Kim HI, Gauthier S, Pellerin L, Hamel E. 2017. [18f]fdg pet signal is driven by astroglial glutamate transport. *Nature Neuroscience* 20:393–395.

UNIVERSITY
OF TURKU

Painosalama Oy, Turku, Finland 2020

ISBN 978-951-29-8150-2 (PRINT)
ISBN 978-951-29-8151-9 (PDF)
ISSN 0355-9483 (Print)
ISSN 2343-3213 (Online)